第5章　图像复原与重建

- 数字图象恢复与增强的目的类似，也是旨在改善图象的质量.
- 但恢复是力求保持图象的本来面目，即以**保真**原则为其前提，这是区别于增强的基本不同点。
- 因而恢复时要了解图象质量下降的物理过程，找出或估计其物理模型。恢复的过程就是沿着质量下降的逆过程来重现原始图象.

第5章　图像复原与重建

5.1　图像退化/复原过程的模型
5.2　噪声模型
5.3　只存在噪声的复原——空间滤波
5.4　用频率域消除周期噪声
5.5　线性、位置不变的退化
5.6　估计退化函数
5.7　逆滤波
5.8　最小均方误差（维纳）滤波
5.9　约束最小二乘方滤波
5.10　由投影重建图像

第5章　图像复原与重建

5.1 图像退化/复原过程的模型

- 线性位移不变系统，加性噪声

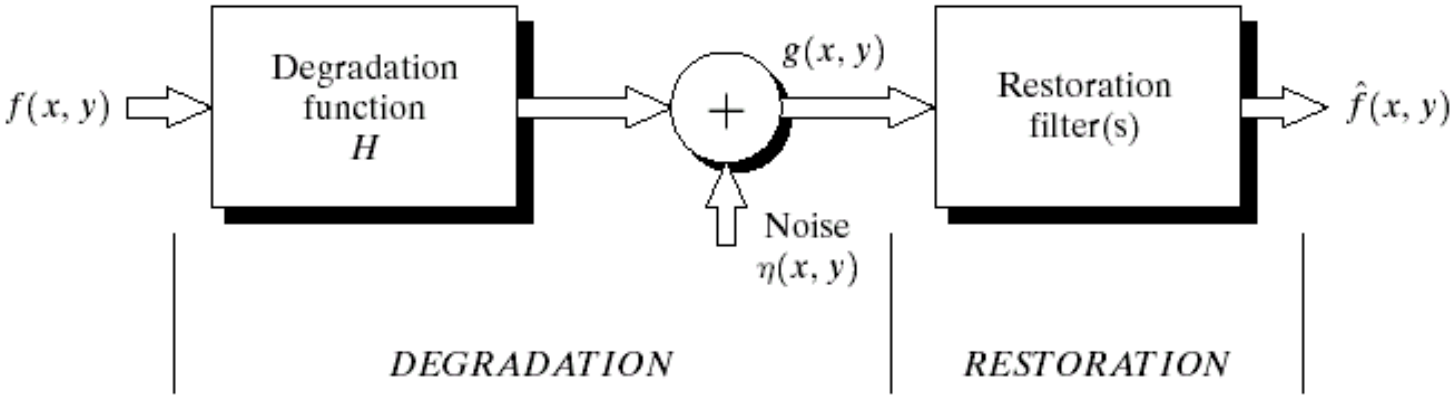

FIGURE 5.1 A model of the image degradation/restoration process.

$$g(x,y) = h(x,y) * f(x,y) + \eta(x,y)$$

$$G(u,v) = H(u,v)F(u,v) + N(u,v)$$

第5章　图像复原与重建

5.1　图像退化/复原过程的模型

5.2　噪声模型

5.3　只存在噪声的复原——空间滤波

5.4　用频率域消除周期噪声

5.5　线性、位置不变的退化

5.6　估计退化函数

5.7　逆滤波

5.8　最小均方误差（维纳）滤波

5.9　约束最小二乘方滤波

5.10　由投影重建图像

5.2 噪声模型

- 噪声的产生
  - 图像获取：CCD相机
  - 图像传输：无线传输
- 噪声的空域特性和频域特性
  - 空域特性：噪声的直方图分布
  - 频域特性：噪声在Fourier频谱上的分布
- 几种典型的噪声模型
  - 高斯噪声（Gaussian noise), 瑞利噪声(Rayleigh noise), 厄兰噪声(Erlang noise), 指数噪声(Exponential noise), 均匀噪声(Uniform noise), 椒盐噪声(salt-and-pepper),

几种典型的噪声模型

$$p(z)=\frac{1}{\sqrt{2\pi}\sigma}e^{-(z-\mu)^2/2\sigma^2}$$ （高斯噪声）

$$p(z)=\begin{cases}\frac{2}{b}(z-a)e^{-(z-a)^2/b} & for\ z\geq a\\ 0 & for\ z<a\end{cases}$$ (瑞利噪声)

$$p(z)=\begin{cases}\frac{a^b z^{b-1}}{(b-1)!}e^{-az} & for\ z\geq 0\\ 0 & for\ z<0\end{cases}$$ (厄兰噪声)

$$p(z)=\begin{cases}ae^{-az} & for\ z\geq 0\\ 0 & for\ z<0\end{cases}$$ (指数噪声)

$$p(z)=\begin{cases}\frac{1}{b-a} & if\ a\leq z\leq b\\ 0 & otherwise\end{cases}$$ (均匀噪声)

$$p(z)=\begin{cases}p_a & for\ z=a\\ p_b & for\ z=b\\ 0 & otherwise\end{cases}$$ (椒盐噪声)

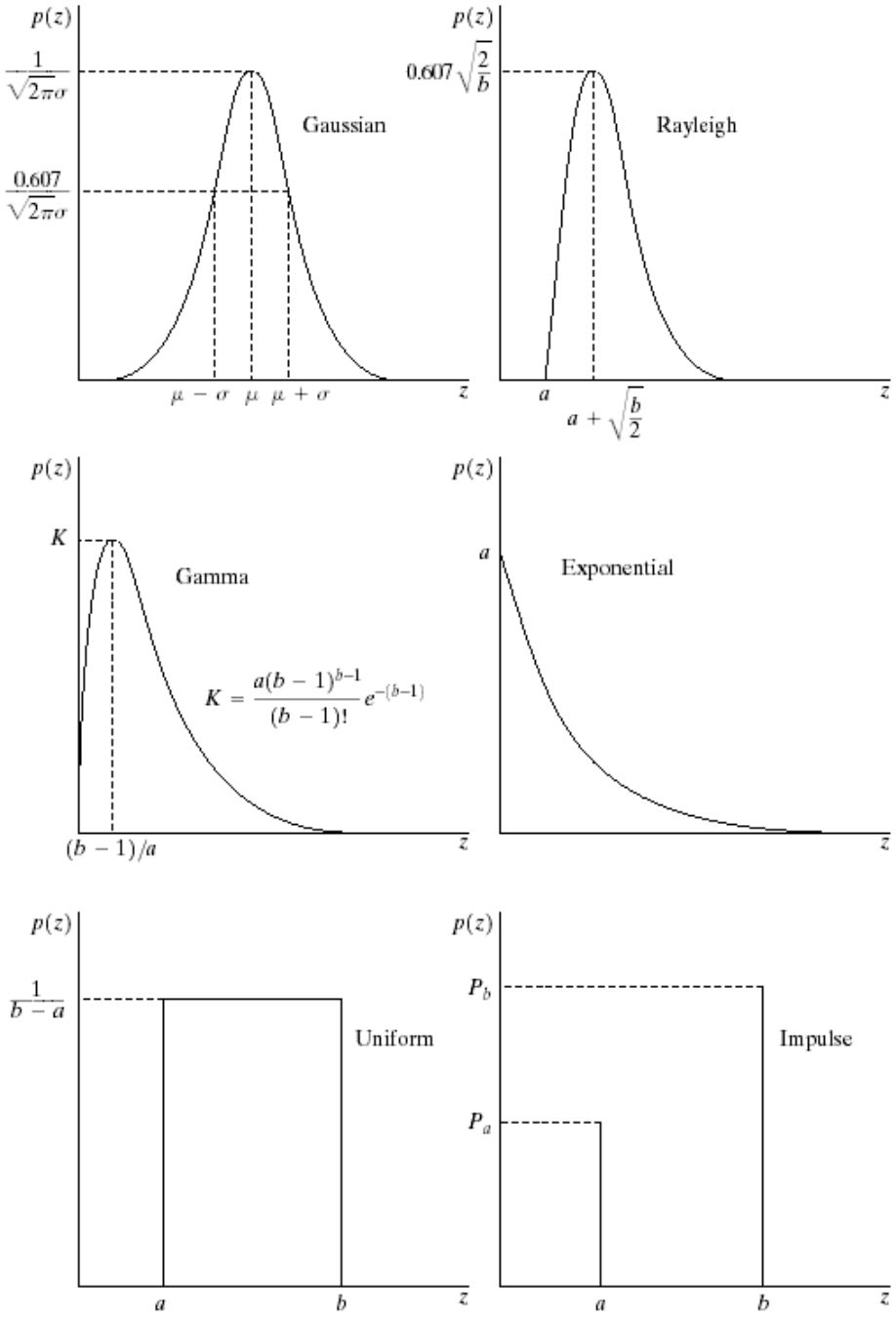
p(z)
1/√(2πσ)
0.607/√(2πσ)
Gaussian
μ − σ
μ
μ + σ
z
p(z)
0.607√(2/b)
Rayleigh
a
a + √(b/2)
z
p(z)
K
Gamma
K = a(b − 1)^{b−1}/(b − 1)! e^{−(b−1)}
(b − 1)/a
z
p(z)
a
Exponential
z
p(z)
1/(b − a)
Uniform
a
b
z
p(z)
P_b
P_a
Impulse
a
b
z

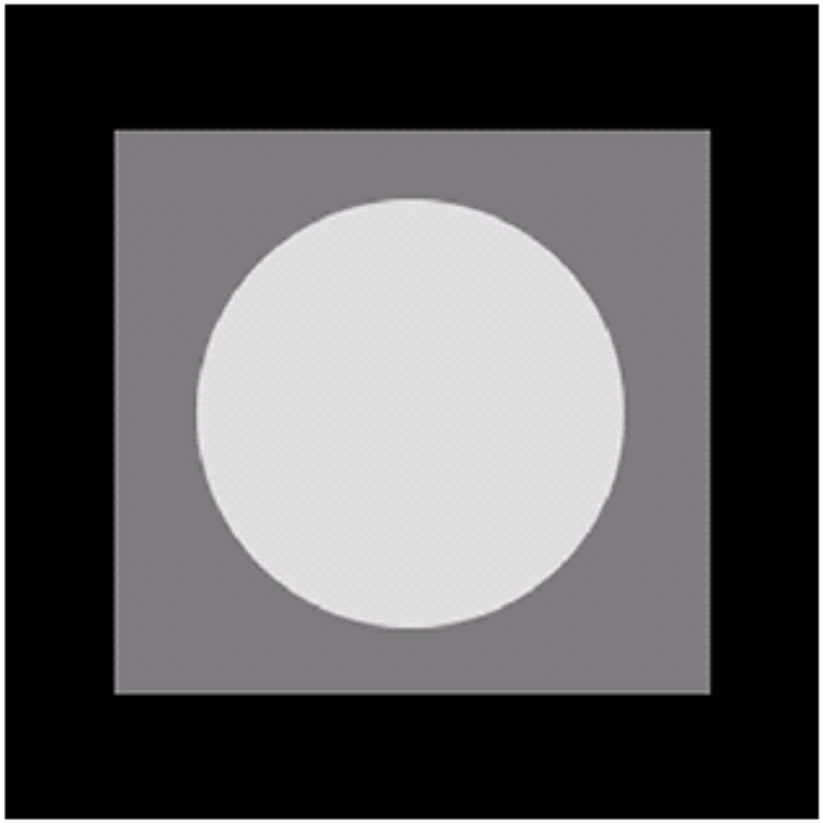

FIGURE 5.3 Test pattern used to illustrate the characteristics of the noise PDFs shown in Fig. 5.2.

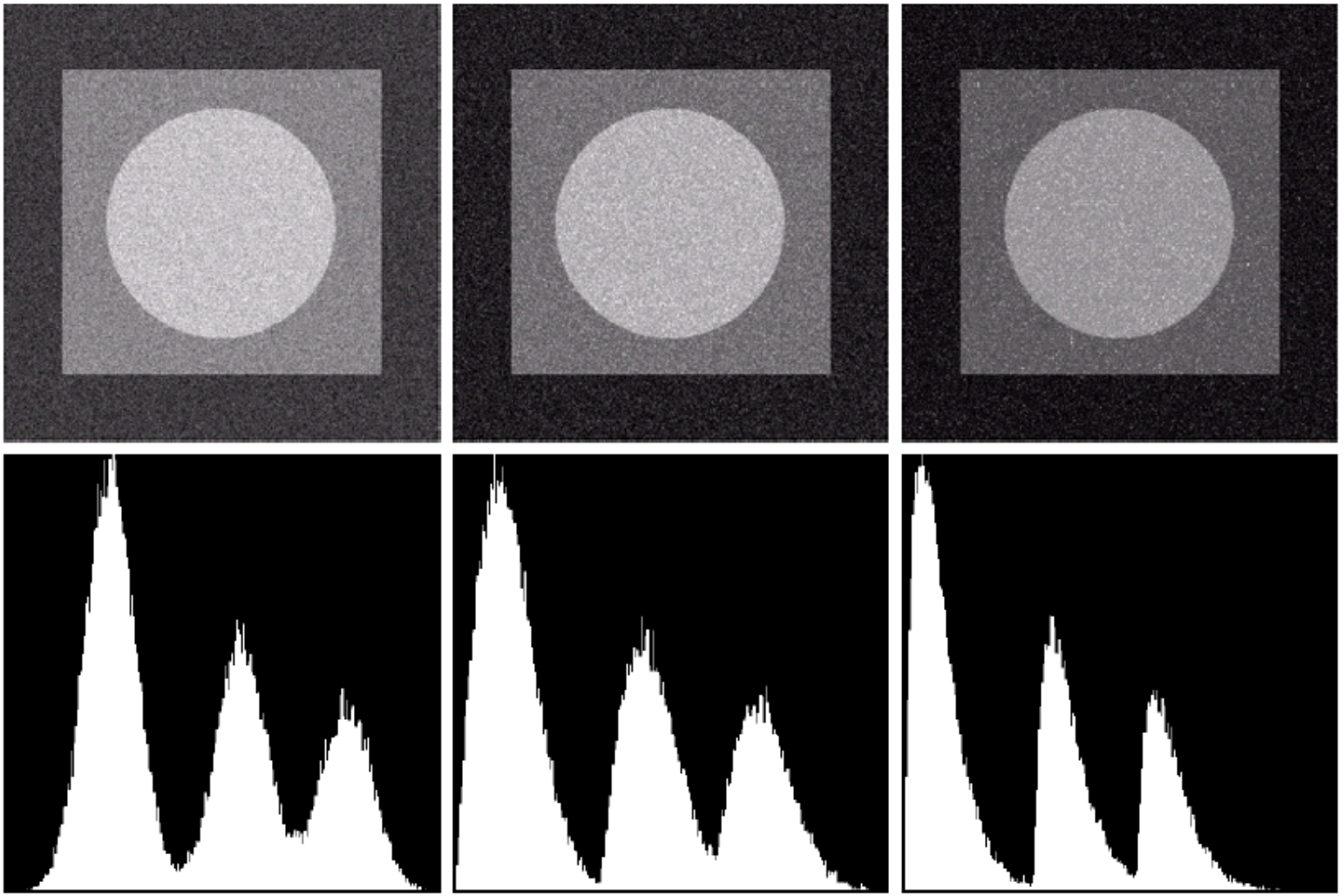

a b c
d e f

FIGURE 5.4 Images and histograms resulting from adding Gaussian, Rayleigh, and gamma noise to the image in Fig. 5.3.

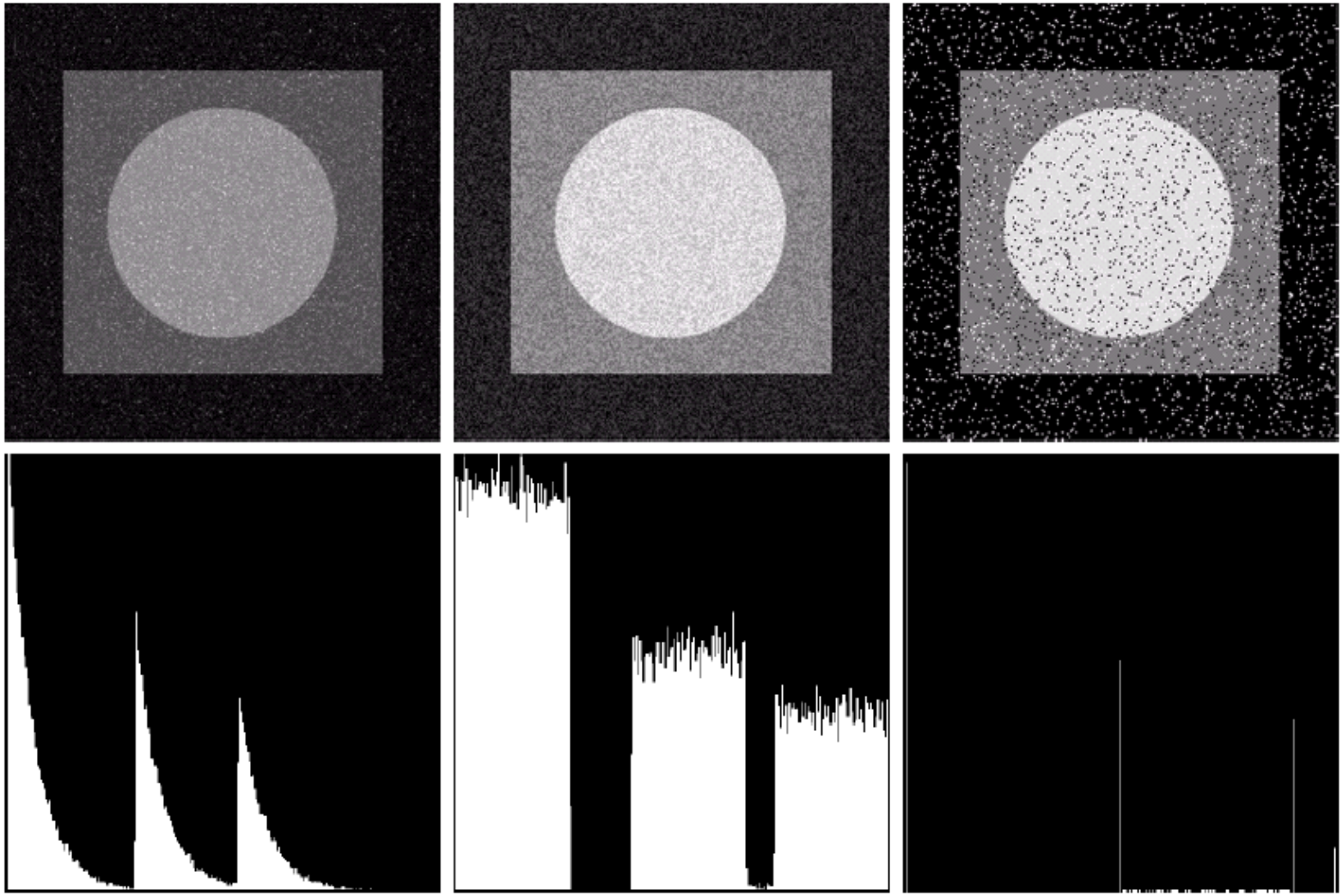

g h i
j k l

FIGURE 5.4 *(Continued)* Images and histograms resulting from adding exponential, uniform, and impulse noise to the image in Fig. 5.3.

周期噪声(Periodic Noise)

a
b

FIGURE 5.5
(a) Image corrupted by sinusoidal noise. (b) Spectrum (each pair of conjugate impulses corresponds to one sine wave). (Original image courtesy of NASA.)

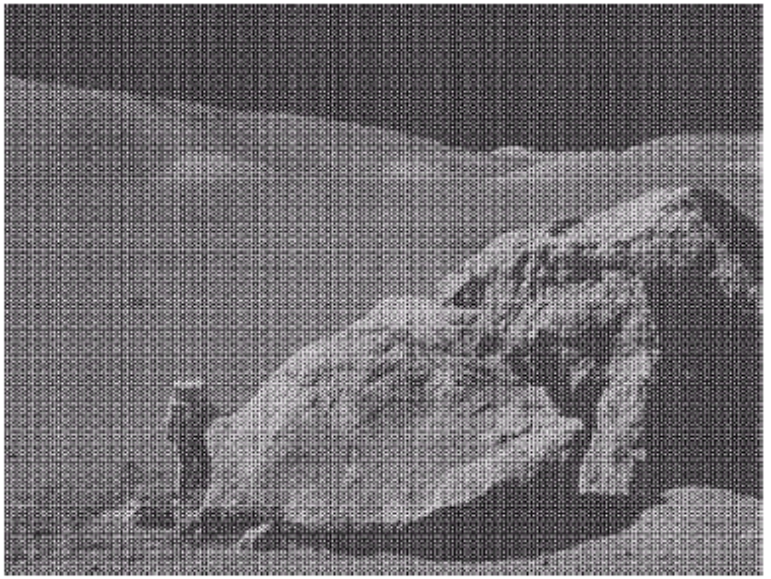

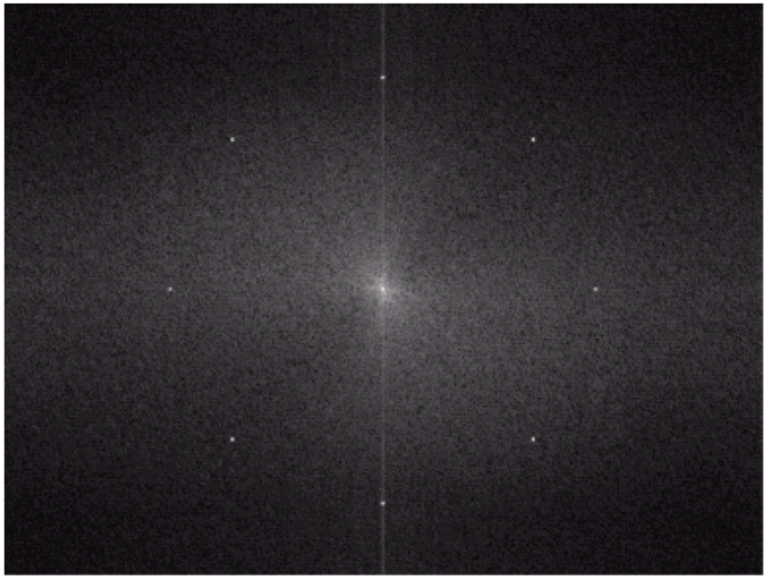

$$\cos(2\pi u_0 x + 2\pi v_0 x)$$

$$\frac{1}{2}[\delta(u + Mu_0, v + Nv_0) + \delta(u - Mu_0, v - Nv_0)]$$

估计噪声参数

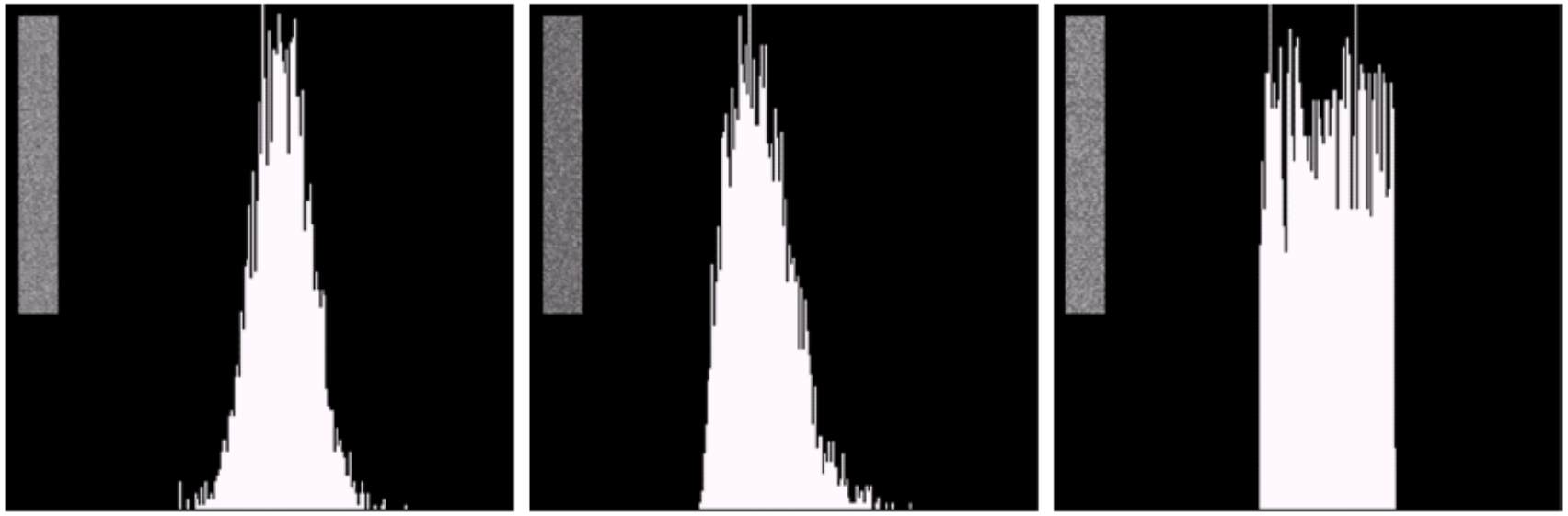

a b c

FIGURE 5.6 Histograms computed using small strips (shown as inserts) from (a) the Gaussian, (b) the Rayleigh, and (c) the uniform noisy images in Fig. 5.4.

第5章　图像复原与重建

5.1　图像退化/复原过程的模型
5.2　噪声模型
5.3　只存在噪声的复原——空间滤波
5.4　用频率域消除周期噪声
5.5　线性、位置不变的退化
5.6　估计退化函数
5.7　逆滤波
5.8　最小均方误差（维纳）滤波
5.9　约束最小二乘方滤波
5.10　由投影重建图像

5.3 只存在噪声的复原——空间滤波

- 基于空域滤波的方法仅针对加性噪声
- 与空域增强原理相同
- 几种常用滤波器
  - 均值滤波器（Mean Filters)
  - 次序统计滤波器（Order Statistic Filters)
  - 自适应滤波器(Adaptive Filters)

几种常用滤波器

- 算术平均滤波器(Arithmetic mean filters)

$$\hat{f}(x,y)=\frac{1}{mn}\sum_{(s,t)\in S_{xy}} g(s,t)$$

- 几何平均滤波器(Geometric mean filter)

$$\hat{f}(x,y)=\left[\prod_{(s,t)\in S_{xy}} g(s,t)\right]^{\frac{1}{mn}}$$

- 调和平均滤波器(Harmonic mean filter)

$$\hat{f}(x,y)=\frac{mn}{\sum_{(s,t)\in S_{xy}} \frac{1}{g(s,t)}}$$

- 反调和平均滤波器(Contraharmonic filter)

$$\hat{f}(x,y)=\frac{\sum_{(s,t)\in S_{xy}} g(s,t)^{Q+1}}{\sum_{(s,t)\in S_{xy}} g(s,t)^{Q}}$$

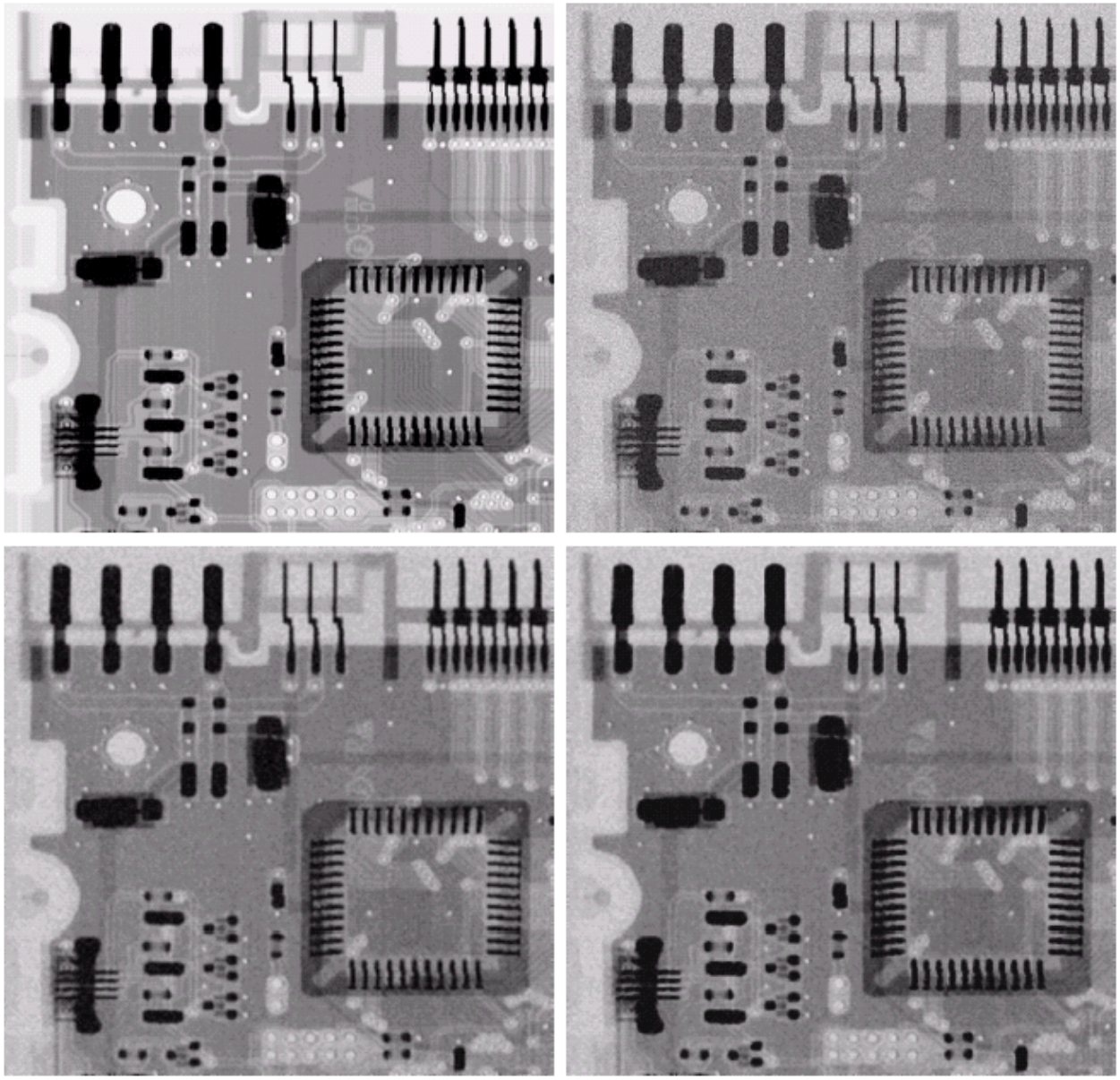

a b
c d

FIGURE 5.7 (a) X-ray image. (b) Image corrupted by additive Gaussian noise. (c) Result of filtering with an arithmetic mean filter of size 3×3. (d) Result of filtering with a geometric mean filter of the same size. (Original image courtesy of Mr. Joseph E. Pascente, Lixi, Inc.)

a b
c d

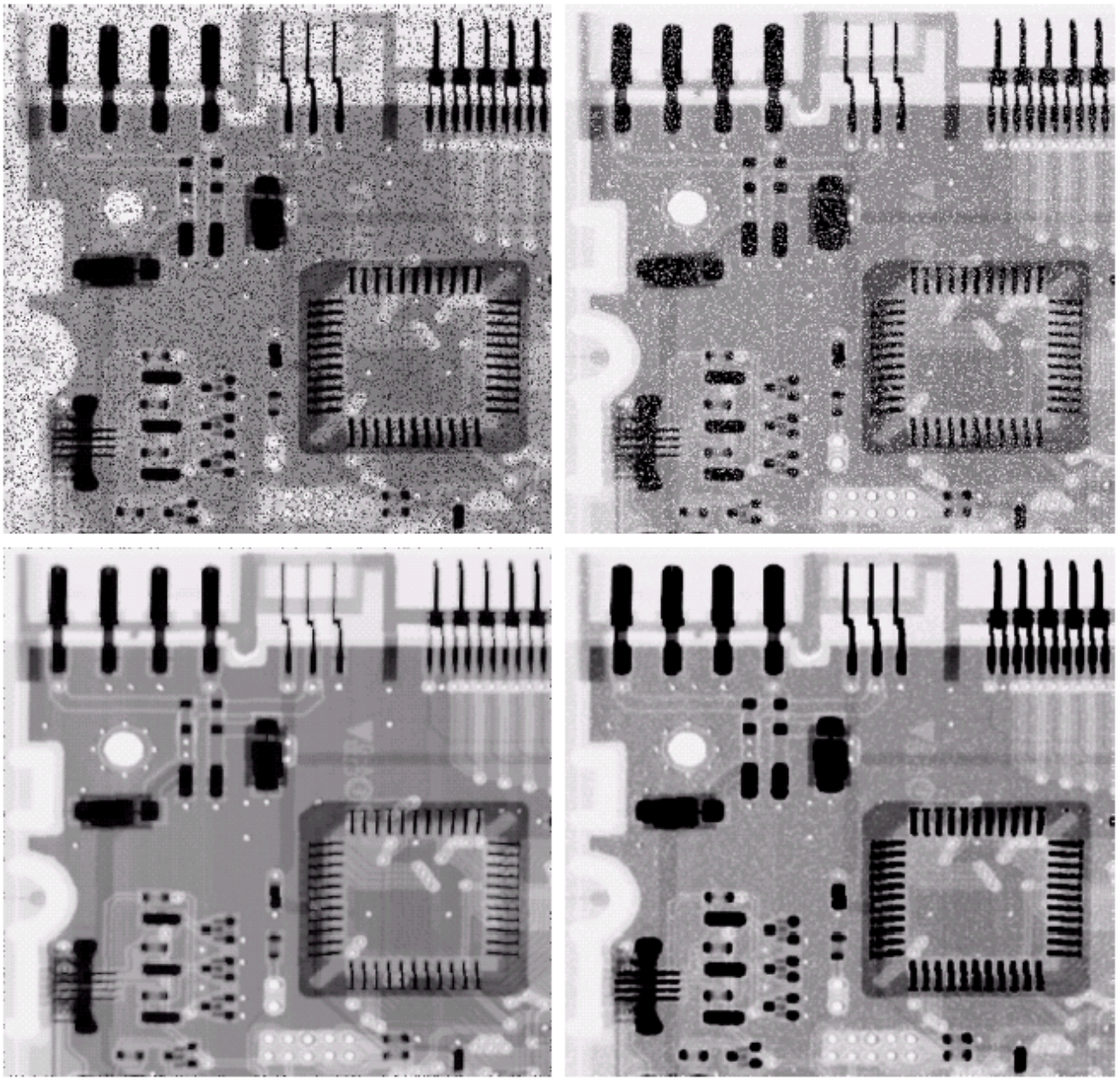

FIGURE 5.8
(a) Image corrupted by pepper noise with a probability of 0.1. (b) Image corrupted by salt noise with the same probability. (c) Result of filtering (a) with a 3×3 contraharmonic filter of order 1.5. (d) Result of filtering (b) with $Q = -1.5$.

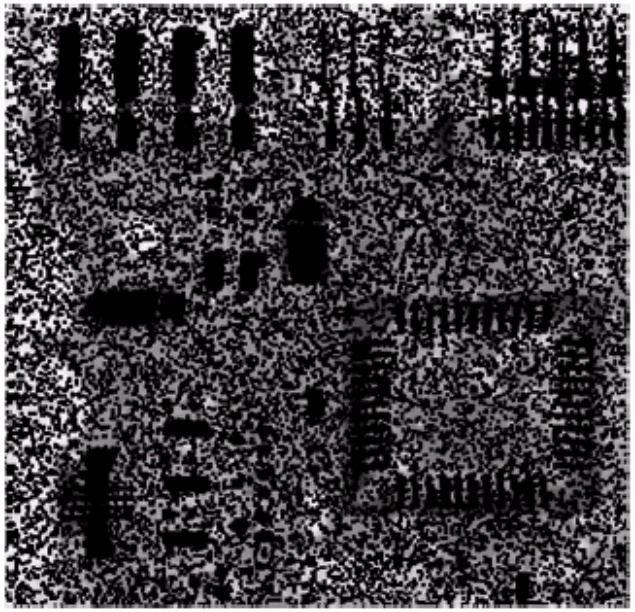

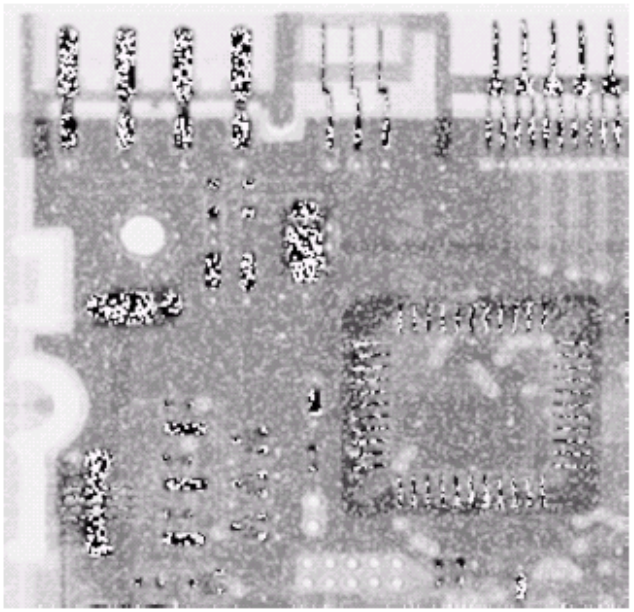

a b

FIGURE 5.9 Results of selecting the wrong sign in contraharmonic filtering. (a) Result of filtering Fig. 5.8(a) with a contraharmonic filter of size 3×3 and $Q = -1.5$. (b) Result of filtering 5.8(b) with $Q = 1.5$.

次序统计滤波器

中值滤波器(Median filter)

$$\hat{f}(x,y)=\underset{(s,t)\in S_{xy}}{median}\{g(s,t)\}$$

最大最小滤波器(Max and min filters)

$$\begin{cases}\hat{f}(x,y)=\max\limits_{(s,t)\in S_{xy}}\{g(s,t)\}\\ \hat{f}(x,y)=\min\limits_{(s,t)\in S_{xy}}\{g(s,t)\}\end{cases}$$

中点滤波器(Midpoint filter)

$$\hat{f}(x,y)=\frac{1}{2}\left[\max_{(s,t)\in S_{xy}}\{g(s,t)\}+\min_{(s,t)\in S_{xy}}\{g(s,t)\}\right]$$

Alpha截取中值滤波器(Alpha-trimmed mean filter)

$$\hat{f}(x,y)=\frac{1}{mn-d}\sum_{(s,t)\in S_{xy}}g_r(s,t)$$

a b
c d

FIGURE 5.10
(a) Image corrupted by salt-and-pepper noise with probabilities $P_a = P_b = 0.1$.
(b) Result of one pass with a median filter of size 3×3.
(c) Result of processing (b) with this filter.
(d) Result of processing (c) with the same filter.

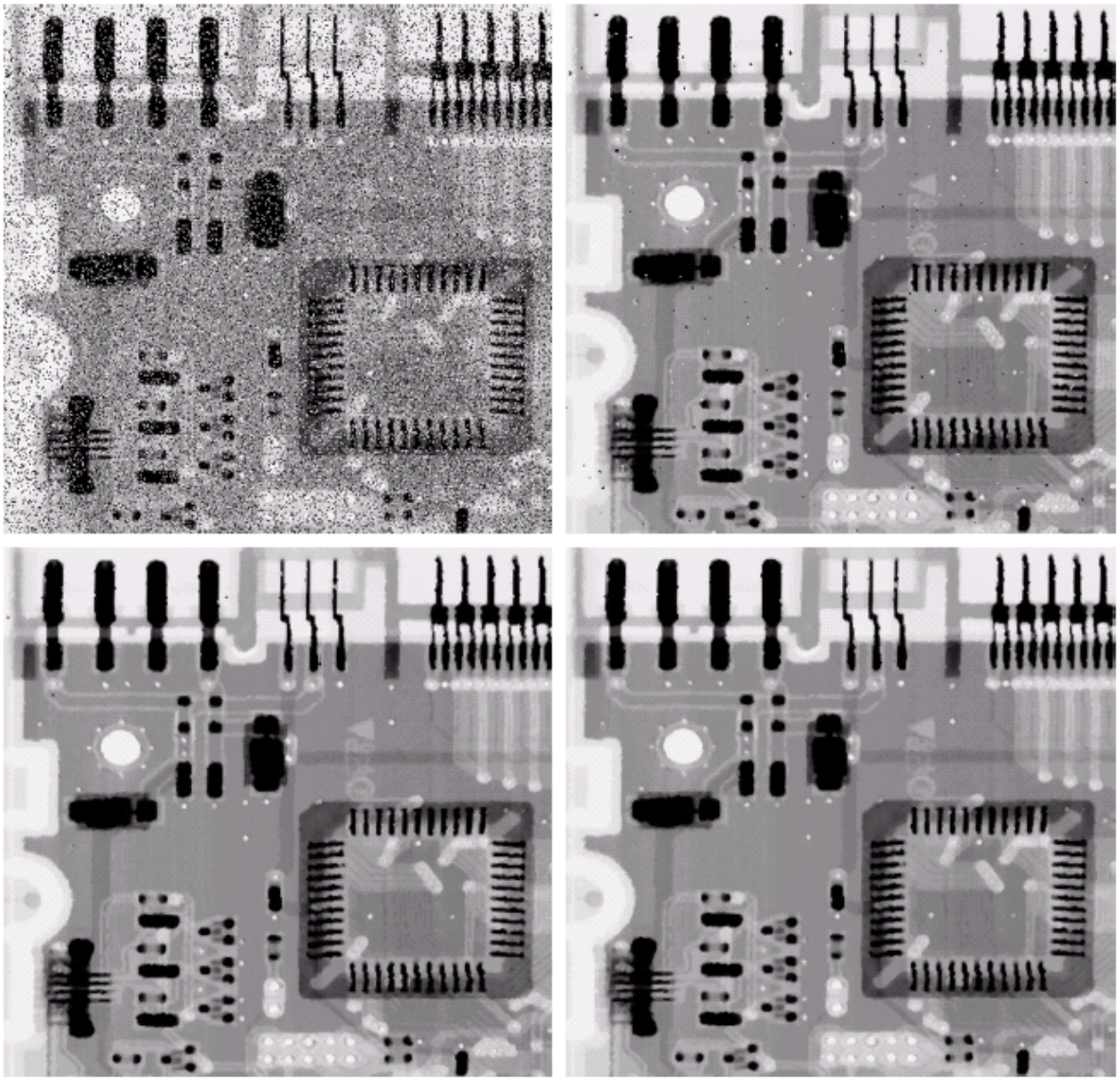

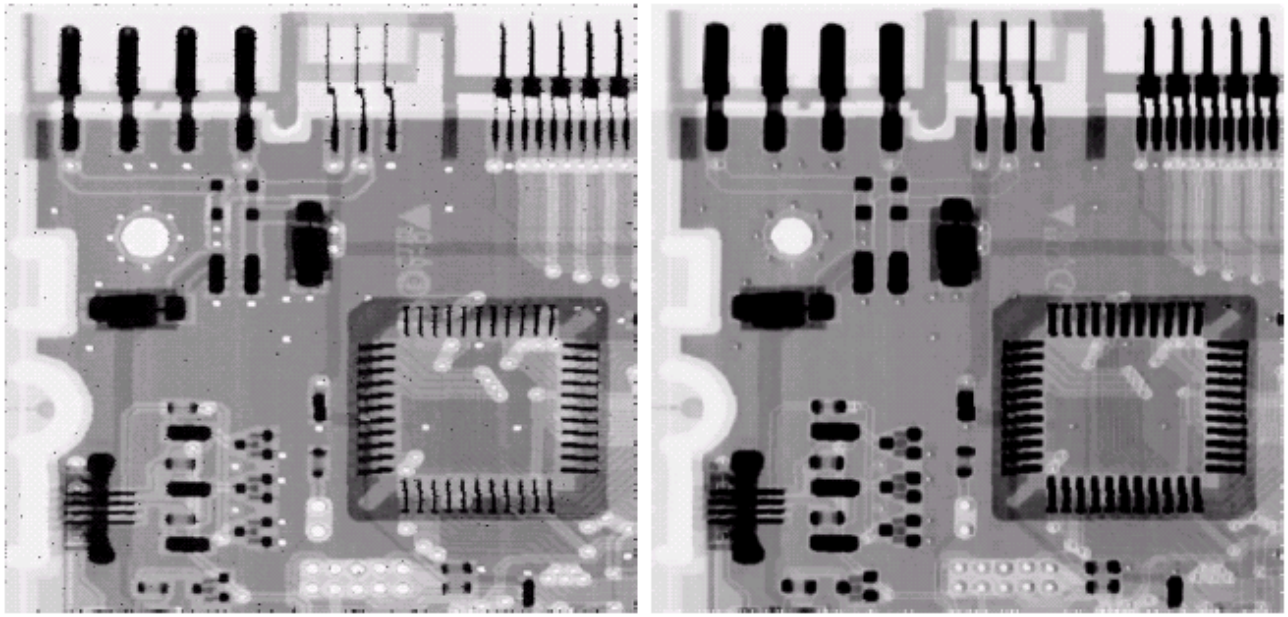

a b

FIGURE 5.11
(a) Result of filtering Fig. 5.8(a) with a max filter of size 3 × 3. (b) Result of filtering 5.8(b) with a min filter of the same size.

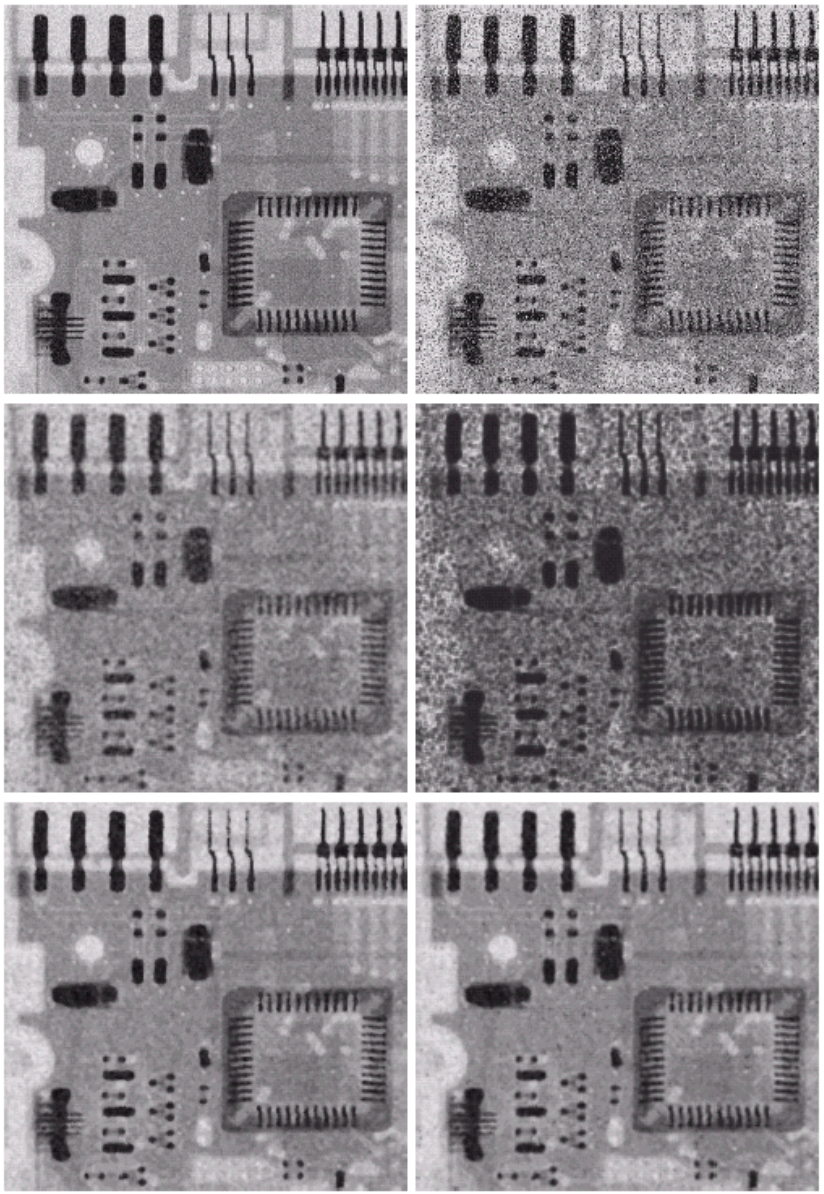

a b
c d
e f

FIGURE 5.12 (a) Image corrupted by additive uniform noise. (b) Image additionally corrupted by additive salt-and-pepper noise. Image in (b) filtered with a 5×5: (c) arithmetic mean filter; (d) geometric mean filter; (e) median filter; and (f) alpha-trimmed mean filter with $d = 5$.

第5章　图像复原与重建

5.1　图像退化/复原过程的模型
5.2　噪声模型
5.3　只存在噪声的复原——空间滤波
5.4　用频率域消除周期噪声
5.5　线性、位置不变的退化
5.6　估计退化函数
5.7　逆滤波
5.8　最小均方误差（维纳）滤波
5.9　约束最小二乘方滤波
5.10　由投影重建图像

5.4 用频率域消除周期噪声

Periodic Noise Reduction by Frequency Domain Filtering

- 带阻滤波器(Bandreject Filters)
- 带通滤波器(Bandpass Filters)
- 槽口滤波器(Notch Filters)

带阻滤波器 (Bandreject Filters)

理想带阻滤波器(Ideal Bandreject Filters)

$$H(u,v)=\begin{cases}1 & if\ D(u,v)<D_0-\dfrac{W}{2}\\ 0 & if\ D_0-\dfrac{W}{2}\le D(u,v)\le D_0+\dfrac{W}{2}\\ 1 & if\ D(u,v)>D_0+\dfrac{W}{2}\end{cases}$$

Butterworth带阻滤波器(Butterworth Bandreject Filters)

$$H(u,v)=\frac{1}{1+\left[\dfrac{D(u,v)W}{D^2(u,v)+D_0^2}\right]^{2n}}$$

高斯带阻滤波器(Gaussian Bandreject Filters)

$$H(u,v)=1-e^{-\frac{1}{2}\left[\frac{D^2(u,v)+D_0^2}{D(u,v)W}\right]^2}$$

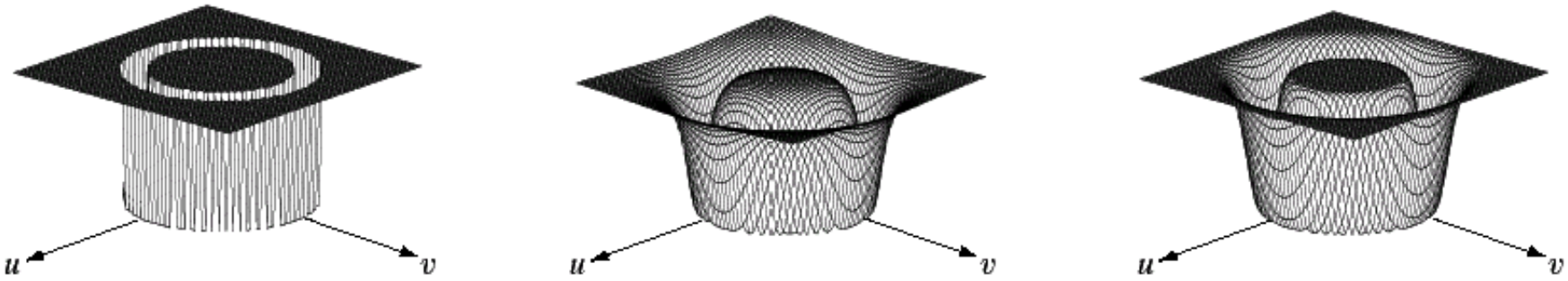

a b c

FIGURE 5.15 From left to right, perspective plots of ideal, Butterworth (of order 1), and Gaussian bandreject filters.

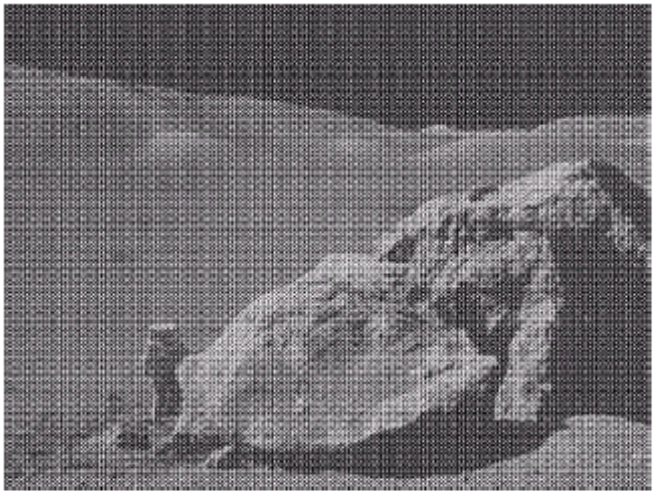

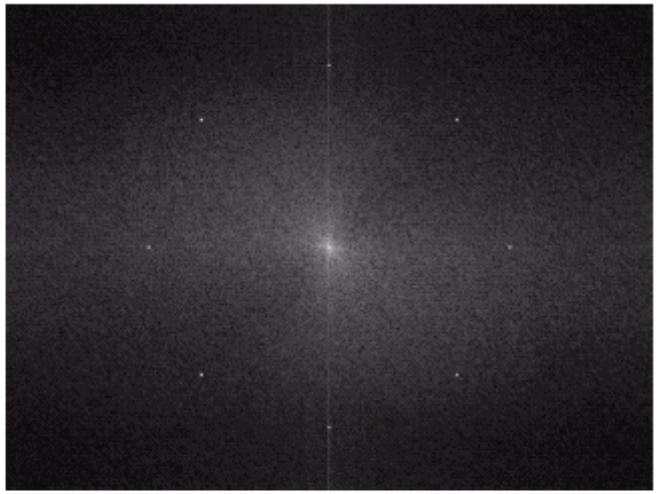

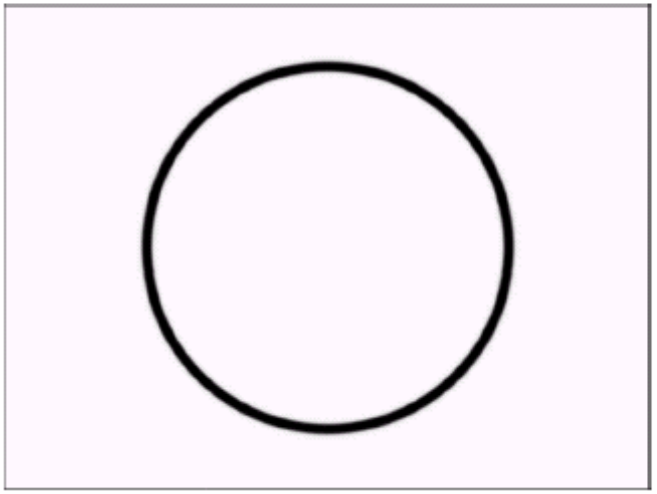

a b
c d

FIGURE 5.16
(a) Image corrupted by sinusoidal noise. (b) Spectrum of (a). (c) Butterworth bandreject filter (white represents 1). (d) Result of filtering. (Original image courtesy of NASA.)

带通滤波器(Bandpass Filters)

带通滤波器与带阻滤波器功能相反

$$H_{bp}(u,v) = 1 - H_{br}(u,v)$$

FIGURE 5.17
Noise pattern of the image in Fig. 5.16(a) obtained by bandpass filtering.

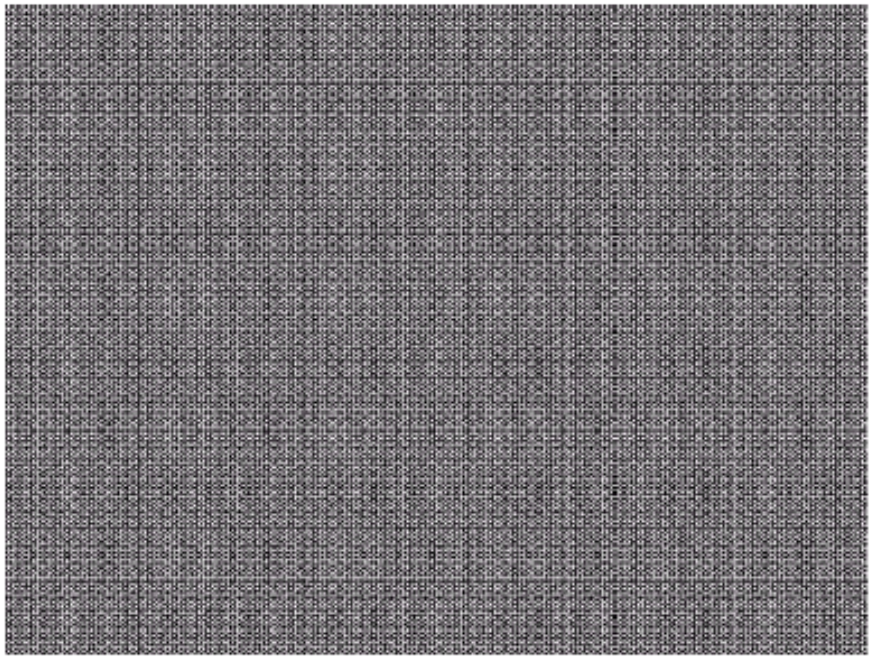

槽口滤波器

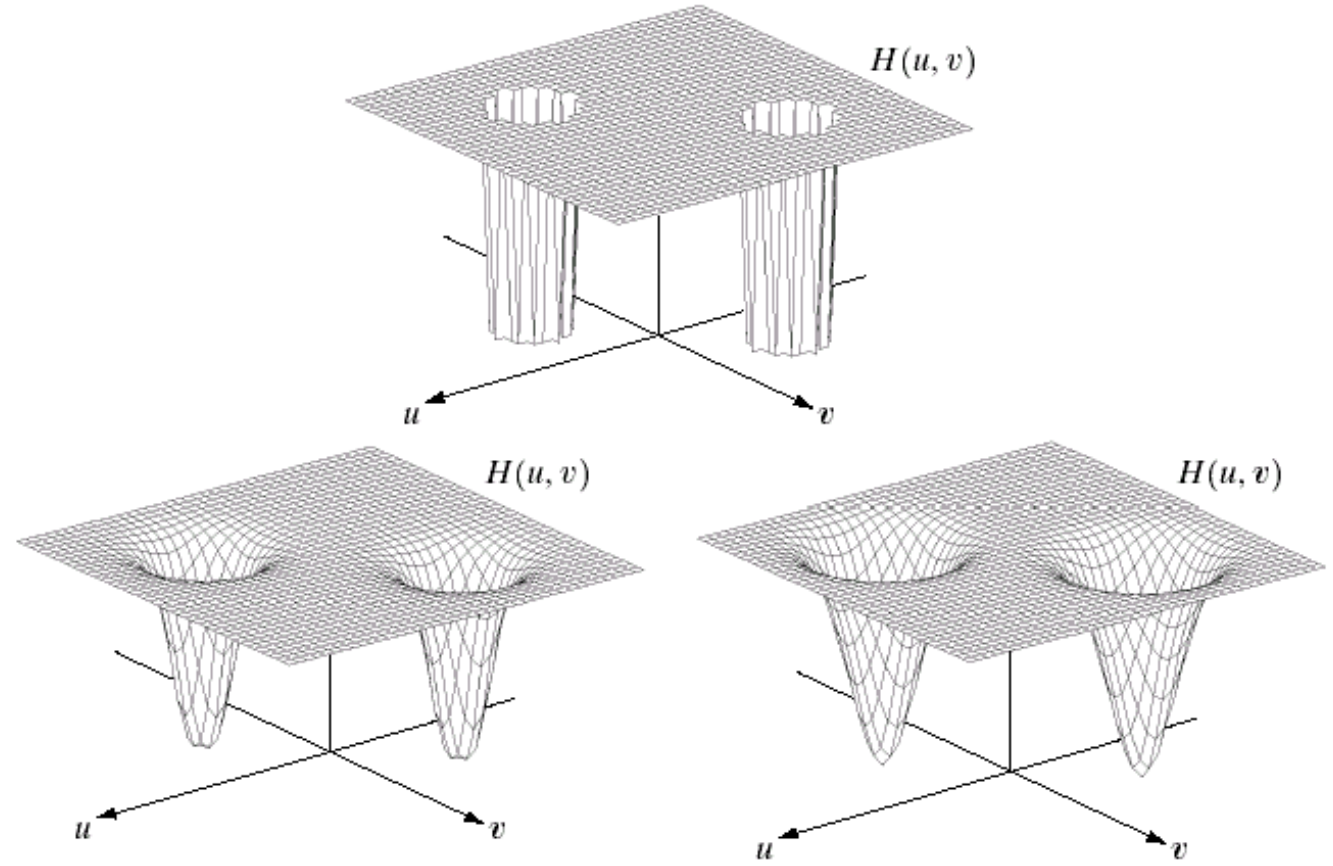

a
b c

FIGURE 5.18 Perspective plots of (a) ideal, (b) Butterworth (of order 2), and (c) Gaussian notch (reject) filters.

a
b c
d e

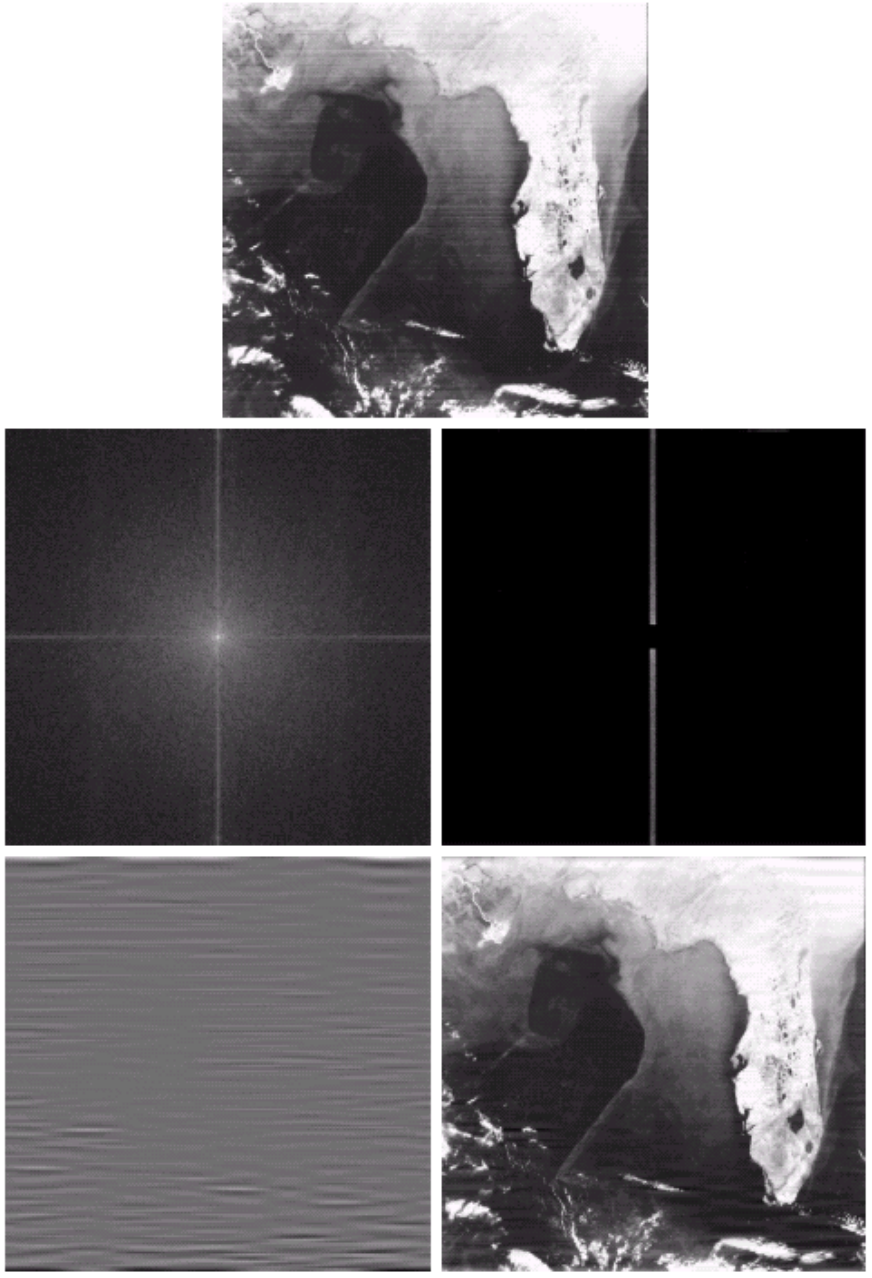

FIGURE 5.19 (a) Satellite image of Florida and the Gulf of Mexico (note horizontal sensor scan lines). (b) Spectrum of (a). (c) Notch pass filter shown superimposed on (b). (d) Inverse Fourier transform of filtered image, showing noise pattern in the spatial domain. (e) Result of notch reject filtering. (Original image courtesy of NOAA.)

第5章　图像复原与重建

5.1　图像退化/复原过程的模型
5.2　噪声模型
5.3　只存在噪声的复原——空间滤波
5.4　用频率域消除周期噪声
5.5　线性、位置不变的退化
5.6　估计退化函数
5.7　逆滤波
5.8　最小均方误差（维纳）滤波
5.9　约束最小二乘方滤波
5.10　由投影重建图像

5.5 线性、位置不变的退化

降质过程：

$$g(x,y)=H[f(x,y)]+\eta(x,y)$$

线性系统：

$$H[af_1(x,y)+bf_2(x,y)]=aH[f_1(x,y)]+bH[f_2(x,y)]$$

位置不变系统：

$$H[f(x-\alpha,y-\beta)]=g(x-\alpha,y-\beta)$$

线性位置不变降质模型

$$g(x,y)=h(x,y)*f(x,y)+\eta(x,y)$$

$$G(u,v)=H(u,v)F(u,v)+N(u,v)$$

第5章　图像复原与重建

5.1　图像退化/复原过程的模型
5.2　噪声模型
5.3　只存在噪声的复原——空间滤波
5.4　用频率域消除周期噪声
5.5　线性、位置不变的退化
5.6　估计退化函数
5.7　逆滤波
5.8　最小均方误差（维纳）滤波
5.9　约束最小二乘方滤波
5.10　由投影重建图像

5.6 估计退化函数

Estimating the Degradation Function

- 通过观测图像估计(Estimation by Image Observation)
- 通过实验估计(Estimation by Experimentation)
- 通过数学建模估计(Estimation by Modeling)

图像观测估计

- 假设：退化过程为线性、位置不变的
- 通过图像本身收集信息来估计退化函数H
  - 从图像中选取有很强信号内容的区域（高对比度）
  - 对该图像进行处理，得到尽可能不模糊的结果
    - ✓ 如锐化处理、甚至手工方法处理
  - 基于处理之后的图像频谱，估计退化函数频谱

$$H(u,v) = \frac{G(u,v)}{F(u,v)}$$

试验估计

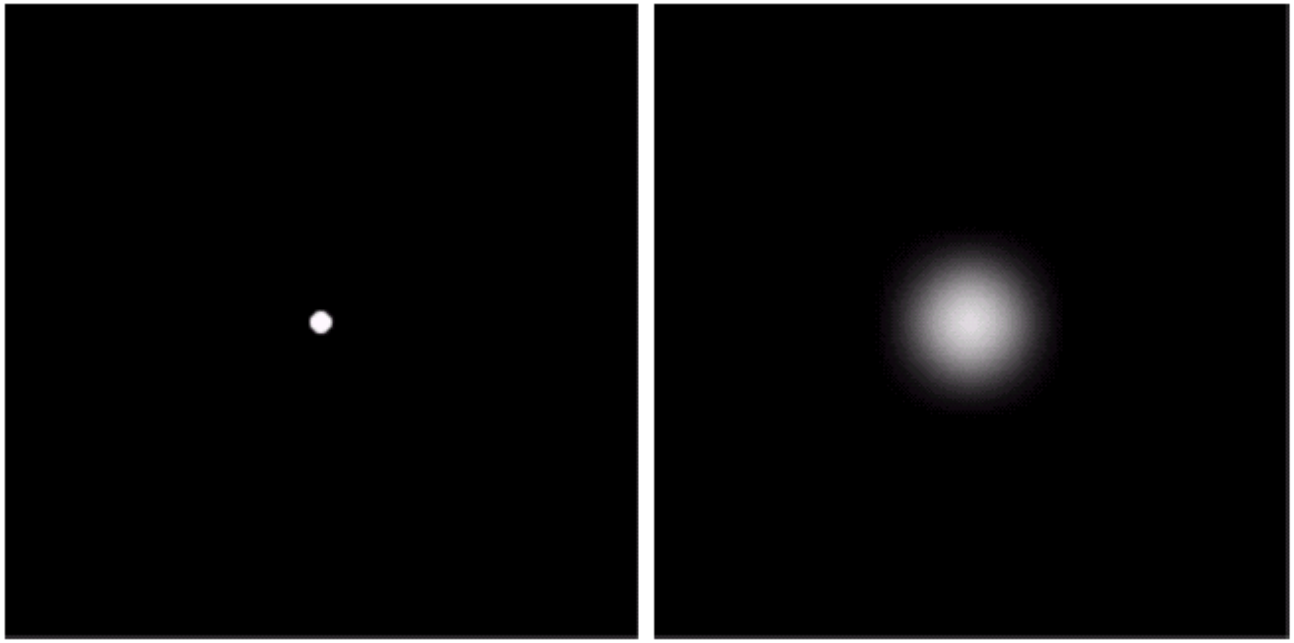

a b

FIGURE 5.24 Degradation estimation by impulse characterization. (a) An impulse of light (shown magnified). (b) Imaged (degraded) impulse.

建模估计

a b
c d

FIGURE 5.25
Illustration of the atmospheric turbulence model. (a) Negligible turbulence. (b) Severe turbulence, $k = 0.0025$. (c) Mild turbulence, $k = 0.001$. (d) Low turbulence, $k = 0.00025$. (Original image courtesy of NASA.)

$$H(u,v) = e^{-k(u^2+v^2)^{5/6}}$$

建模估计

- 从基本原理推导数学模型

$$g(x,y)=\int_0^T f\left[x-x_0(\mathrm{t}),y-y_0(\mathrm{t})\right]dt$$

$$H(u,v)=\frac{T}{\pi(ua+vb)}\sin[\pi(ua+vb)]e^{-j\pi(ua+vb)} \qquad x(t)=at/T;\ \ y(t)=bt/T$$

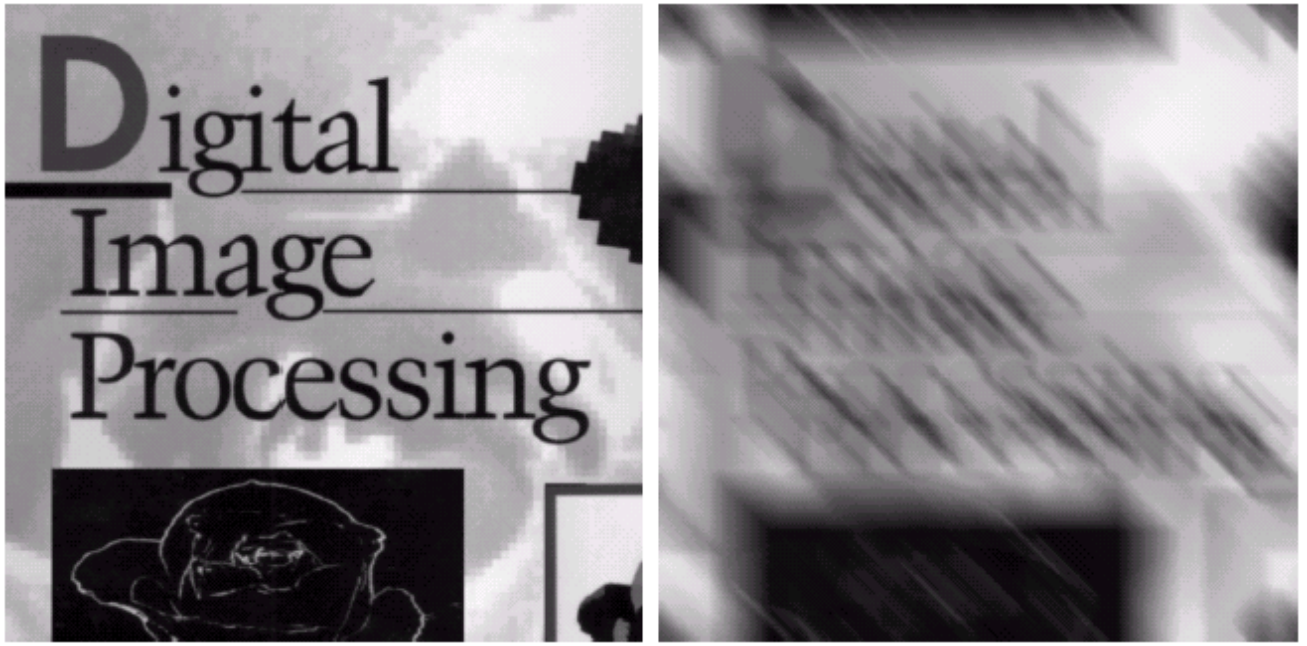

a b

FIGURE 5.26 (a) Original image. (b) Result of blurring using the function in Eq. (5.6-11) with $a = b = 0.1$ and $T = 1$.

第5章　图像复原与重建

5.1　图像退化/复原过程的模型
5.2　噪声模型
5.3　只存在噪声的复原——空间滤波
5.4　用频率域消除周期噪声
5.5　线性、位置不变的退化
5.6　估计退化函数
5.7　逆滤波
5.8　最小均方误差（维纳）滤波
5.9　约束最小二乘方滤波
5.10　由投影重建图像

5.7 逆滤波

- 最简单且粗糙的恢复方法
- 降质图像频谱直接除以降质函数：

$$\hat{F}(u,v)=\frac{G(u,v)}{H(u,v)} \qquad \hat{F}(u,v)=F(u,v)+\frac{N(u,v)}{H(u,v)}$$

- 由于$N(u,v)$未知，即使得到降质函数$H(u,v)$，也难以精确重建
- $H(u,v)$在某些位置为0或者是非常小的值，$F(u,v)$被淹没
  - 解决方法：限制频谱范围

a b
c d

FIGURE 5.27
Restoring Fig. 5.25(b) with Eq. (5.7-1). (a) Result of using the full filter. (b) Result with H cut off outside a radius of 40; (c) outside a radius of 70; and (d) outside a radius of 85.

第5章　图像复原与重建

5.1　图像退化/复原过程的模型
5.2　噪声模型
5.3　只存在噪声的复原——空间滤波
5.4　用频率域消除周期噪声
5.5　线性、位置不变的退化
5.6　估计退化函数
5.7　逆滤波
5.8　最小均方误差（维纳）滤波
5.9　约束最小二乘方滤波
5.10　由投影重建图像

5.8 最小均方误差（维纳）滤波

- 确定未污染图像 f 的一个估计 $\hat{f}$，使得他们之间的均方误差最小

$$e^2 = E\left\{(f - \hat{f})^2\right\}$$

$$F(u,v) = \left[\frac{1}{H(u,v)}\frac{|H(u,v)|^2}{|H(u,v)|^2 + S_\eta(u,v)/S_f(u,v)}\right]G(u,v)$$

$$F(u,v) = \left[\frac{1}{H(u,v)}\frac{|H(u,v)|^2}{|H(u,v)|^2 + K}\right]G(u,v)$$

逆滤波与维纳滤波比较

a b c

FIGURE 5.28 Comparison of inverse- and Wiener filtering. (a) Result of full inverse filtering of Fig. 5.25(b). (b) Radially limited inverse filter result. (c) Wiener filter result.

进一步比较

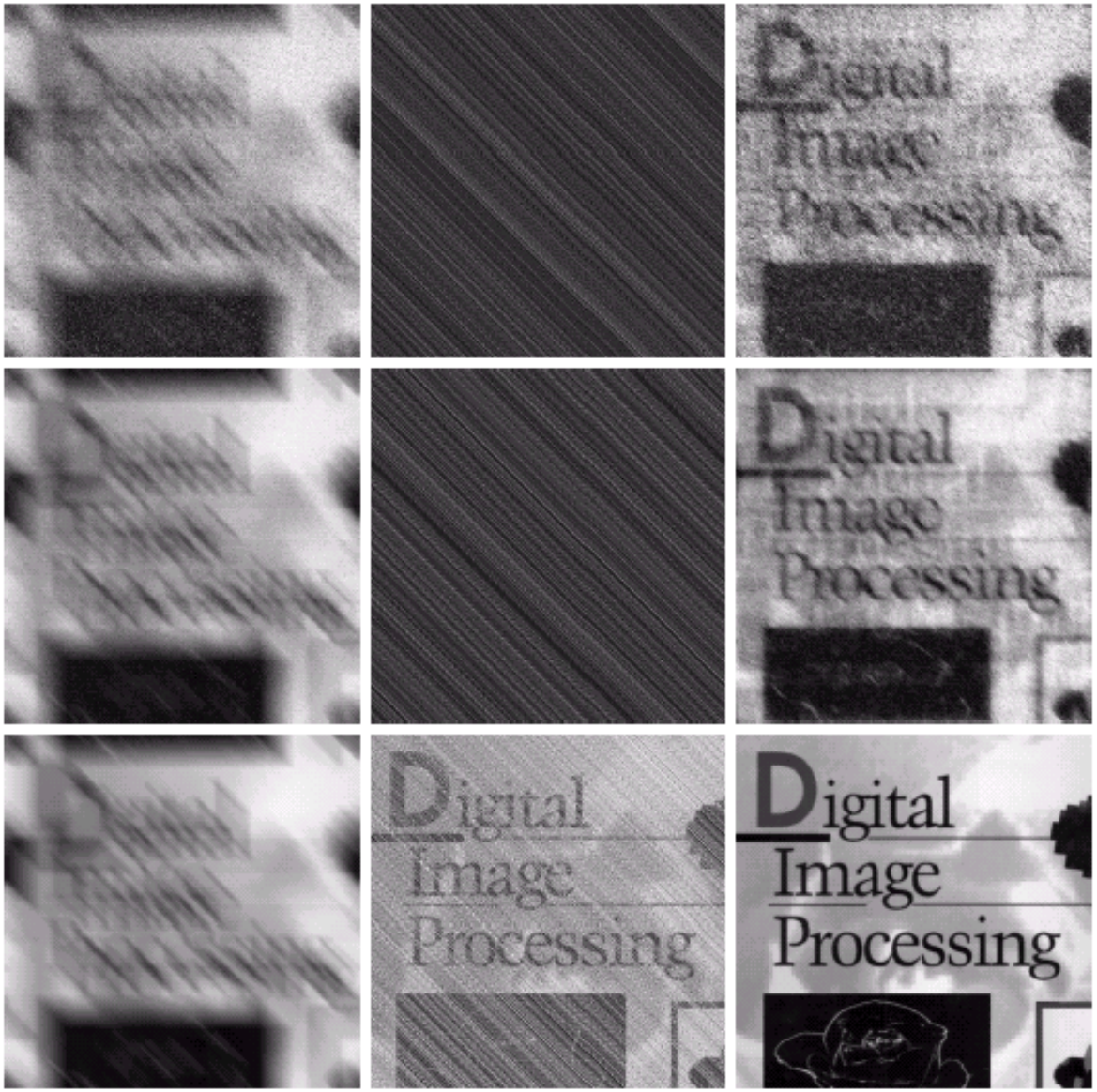

a b c
d e f
g h i

FIGURE 5.29 (a) Image corrupted by motion blur and additive noise. (b) Result of inverse filtering. (c) Result of Wiener filtering. (d)–(f) Same sequence, but with noise variance one order of magnitude less. (g)–(i) Same sequence, but noise variance reduced by five orders of magnitude from (a). Note in (h) how the deblurred image is quite visible through a "curtain" of noise.

第5章　图像复原与重建

5.9 约束最小二乘方滤波

- 与维纳滤波相比
  - 不需要知道信号和噪声的频谱，仅需知道噪声的均值和方差
  - 维纳滤波的最优是平均意义上的，代数法是针对每一幅具体图像

$$g(x,y)=h(x,y)*f(x,y)+\eta(x,y) \quad \Longleftrightarrow \quad g=Hf+\eta$$

$$\begin{bmatrix} 50 & 24 & 33 & 39 \\ 79 & 12 & 14 & 20 \\ 103 & 102 & 98 & 32 \\ 210 & 101 & 19 & 17 \end{bmatrix}$$

$$g, f, \eta : M \times N \Rightarrow MN \times 1$$

$$H : MN \times MN$$

5.9 约束最小二乘方滤波

$$\textbf{min} \quad C = \sum_{x=0}^{M-1}\sum_{y=0}^{N-1}\left[\nabla^2 f(x,y)\right]^2$$

$$\textbf{subject to} \quad \left\|g - H\hat{f}\right\|^2 = \|\eta\|^2 \quad \|\eta\|^2 = MN(\sigma_\eta^2 + \mathrm{m}_\eta^2)$$

$$F(u,v) = \left[\frac{H^*(u,v)}{|H(u,v)|^2 + \gamma|P(u,v)|^2}\right]G(u,v)$$

$$p(\mathrm{x},\mathrm{y}) = \begin{bmatrix} 0 & -1 & 0 \\ -1 & 4 & -1 \\ 0 & -1 & 0 \end{bmatrix} \quad \textbf{FFT} \quad P(\mathrm{u},\mathrm{v})$$

5.9 约束最小二乘方滤波

a b c

FIGURE 5.30 Results of constrained least squares filtering. Compare (a), (b), and (c) with the Wiener filtering results in Figs. 5.29(c), (f), and (i), respectively.

第5章　图像复原与重建

5.10 由投影重建图像

计算机断层(CT)原理

a b
c d e

FIGURE 5.32
(a) Flat region showing a simple object, an input parallel beam, and a detector strip. (b) Result of back-projecting the sensed strip data (i.e., the 1-D absorption profile). (c) The beam and detectors rotated by 90°. (d) Back-projection. (e) The sum of (b) and (d). The intensity where the back-projections intersect is twice the intensity of the individual back-projections.

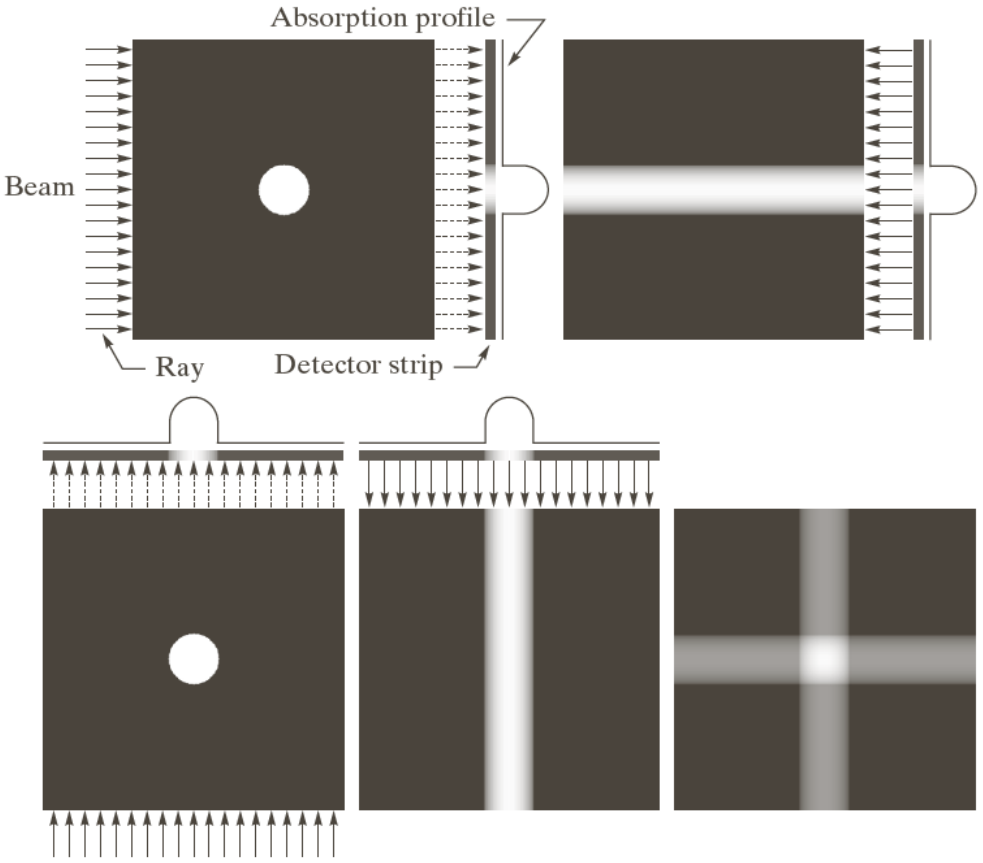

5.10 由投影重建图像

计算机断层(CT)原理

a b c
d e f

FIGURE 5.33
(a) Same as Fig. 5.32(a). (b)–(e) Reconstruction using 1, 2, 3, and 4 backprojections 45° apart. (f) Reconstruction with 32 backprojections 5.625° apart (note the blurring).

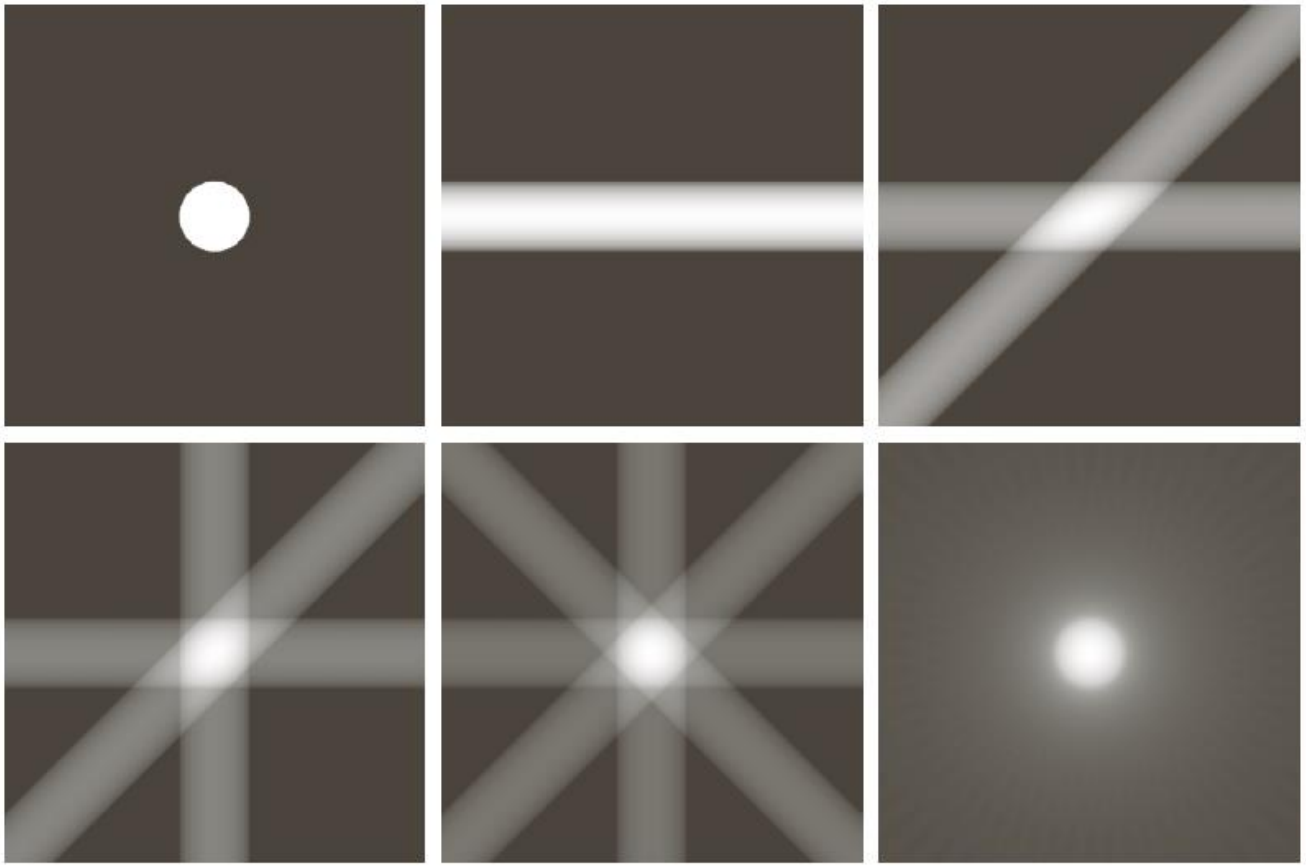

5.10 由投影重建图像

计算机断层(CT)原理

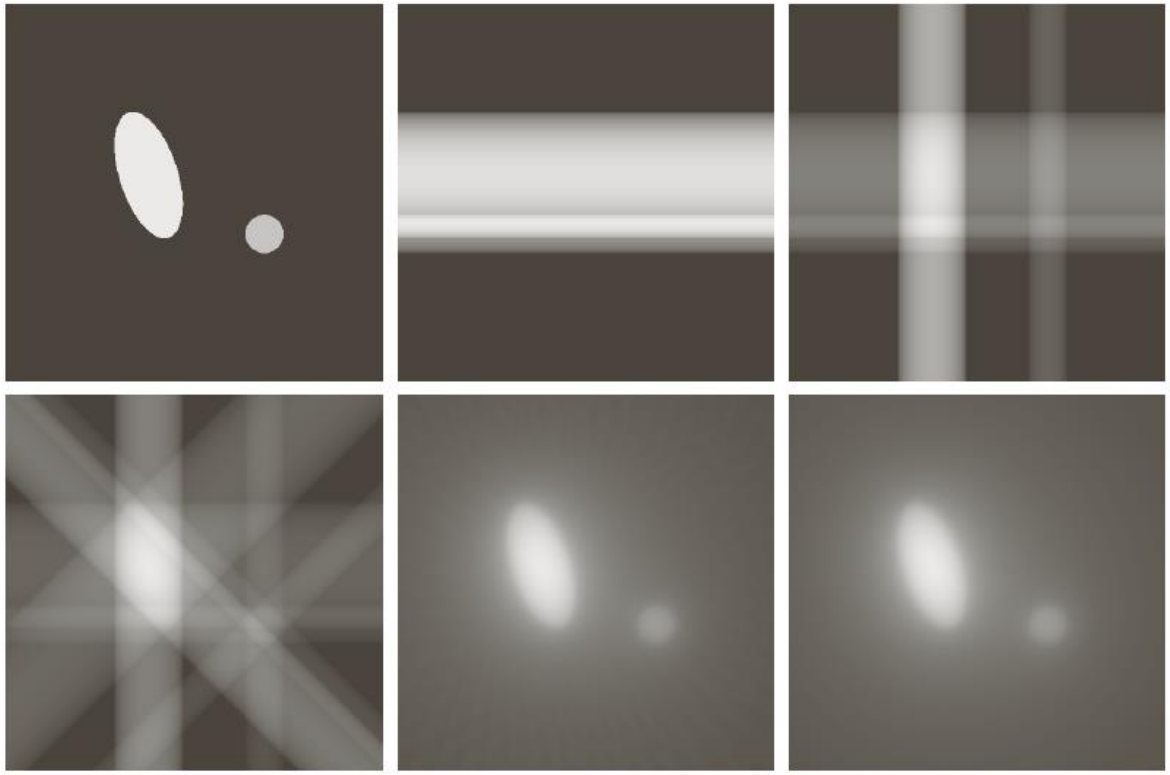

a b c
d e f

FIGURE 5.34 (a) A region with two objects. (b)–(d) Reconstruction using 1, 2, and 4 backprojections 45° apart. (e) Reconstruction with 32 backprojections 5.625° apart. (f) Reconstruction with 64 backprojections 2.8125° apart.

5.10 由投影重建图像

计算机断层(CT)原理

- 1919 Johann Rodon 提出Radon变换
- 1962年Allan M. Cormack, Tuffs Univ. 设计CT原型
- G. N. Hounsfield, 英国伦敦EMI公司工程师，同时设计第一台医用CT
- A. M. Cormack和G. N. Hounsfield获1979年诺贝尔医学奖

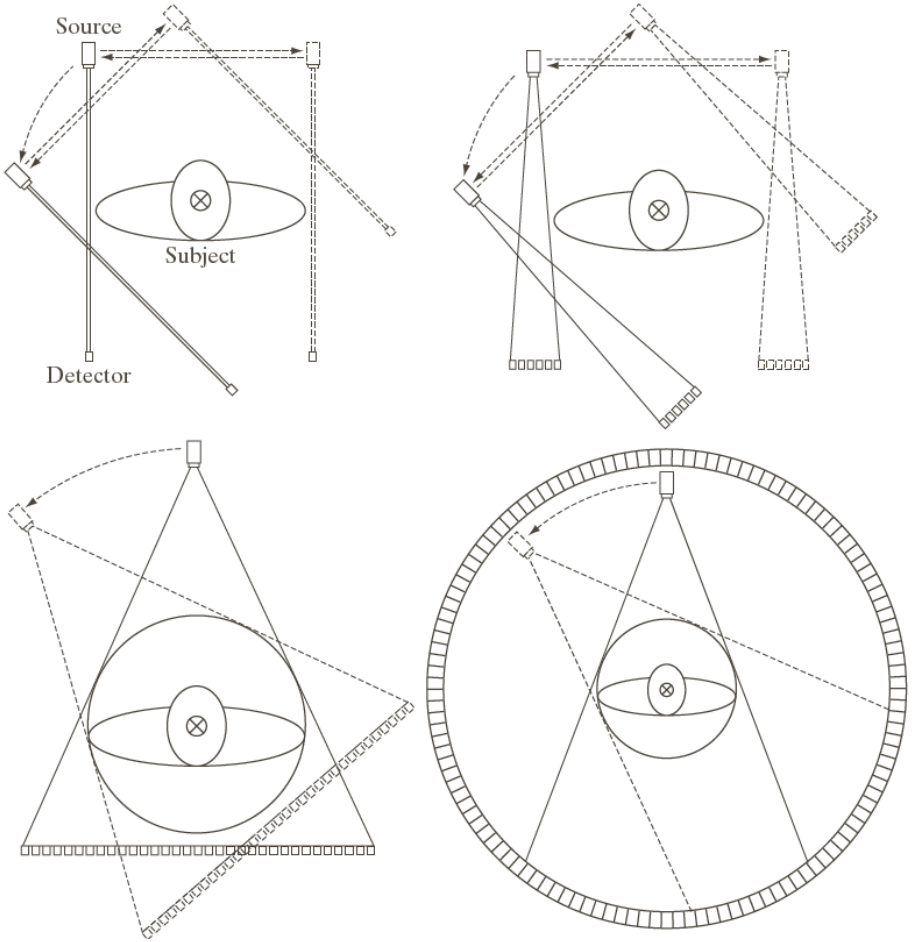

a b
c d

FIGURE 5.35 Four generations of CT scanners. The dotted arrow lines indicate incremental linear motion. The dotted arrow arcs indicate incremental rotation. The cross-mark on the subject's head indicates linear motion perpendicular to the plane of the paper. The double arrows in (a) and (b) indicate that the source/detector unit is translated and then brought back into its original position.

5.10 由投影重建图像

投影和雷登变换(Radon Transform)

$$x\cos\theta + y\sin\theta = \rho$$

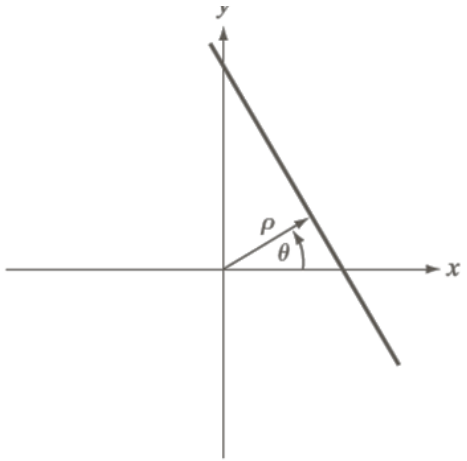

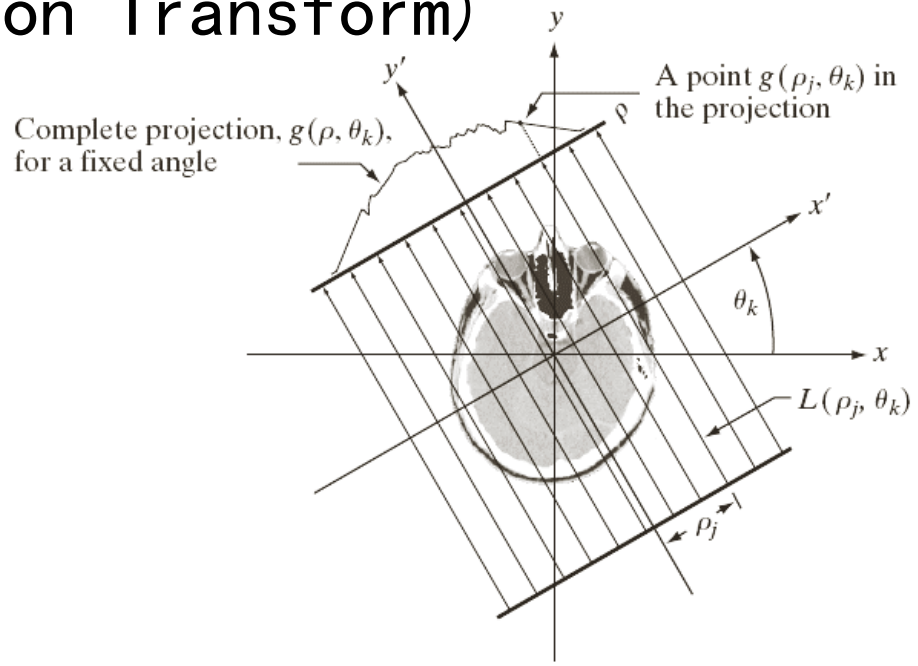

$$g(\rho_j,\theta_k)=\int_{-\infty}^{+\infty}\int_{-\infty}^{+\infty} f(x,y)\delta(x\cos\theta_k + y\sin\theta_k - \rho_j)dxdy$$

$$g(\rho,\theta)=\int_{-\infty}^{+\infty}\int_{-\infty}^{+\infty} f(x,y)\delta(x\cos\theta + y\sin\theta - \rho)dxdy$$

$$g(\rho,\theta)=\sum_{x=0}^{M-1}\sum_{y=0}^{N-1} f(x,y)\delta(x\cos\theta + y\sin\theta - \rho)dxdy$$

5.10 由投影重建图像

正弦图(sinogram)： $g(\rho,\theta)$

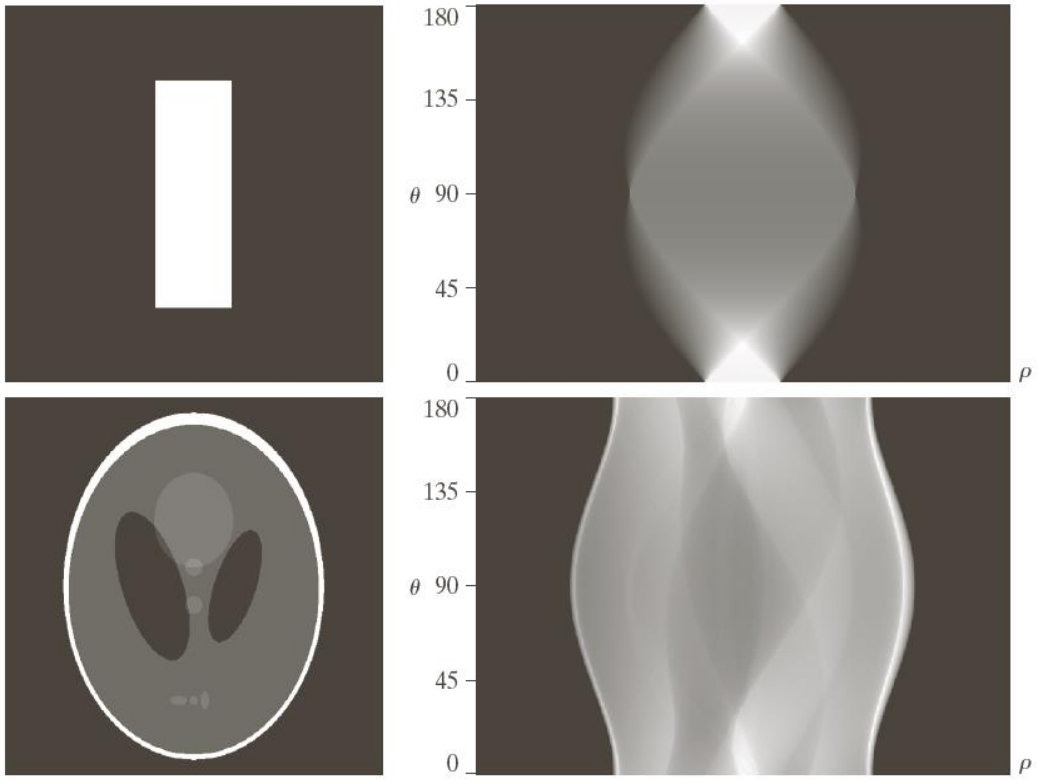

a b
c d

FIGURE 5.39 Two images and their sinograms (Radon transforms). Each row of a sinogram is a projection along the corresponding angle on the vertical axis. Image (c) is called the *Shepp-Logan phantom*. In its original form, the contrast of the phantom is quite low. It is shown enhanced here to facilitate viewing.

5.10 由投影重建图像

从正弦图 $g(\rho,\theta)$ 得到反投影图像

$$f_{\theta_k}(x,y) = g(\rho,\theta_k) = \mathrm{g}(x\cos\theta_k + y\sin\theta_k, \theta_k)dxdy$$

$$f_{\theta}(x,y) = \mathrm{g}(x\cos\theta + y\sin\theta, \theta)dxdy$$

$$f(x,y) = \int_0^{\pi} f_{\theta}(x,y) \qquad f(x,y) = \sum_{\theta=0}^{\pi} f_{\theta}(x,y)$$

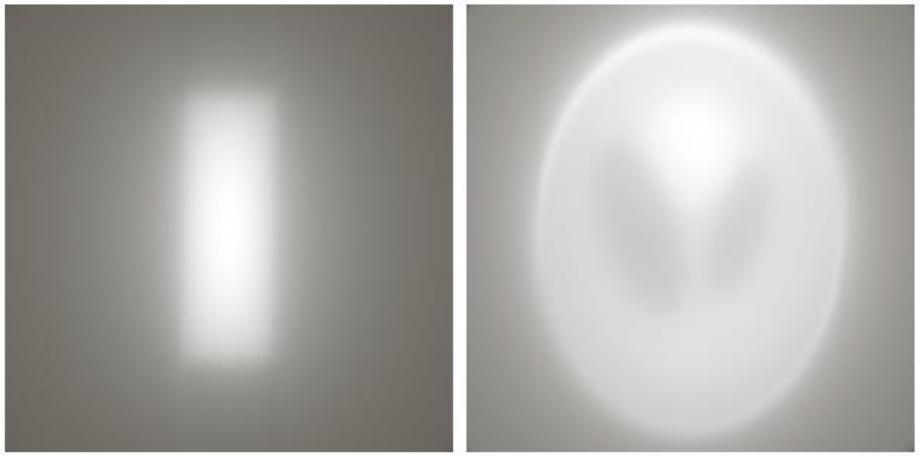

a b

FIGURE 5.40 Backprojections of the sinograms in Fig. 5.39.

5.10 由投影重建图像

傅里叶切片定理

ρ 投影的一维傅里叶变换

$$
\begin{aligned}
G(\omega,\theta) &= \int_{-\infty}^{+\infty} g(\rho,\theta)e^{-j2\pi\omega\rho}d\rho \\
&= \int_{-\infty}^{+\infty}\int_{-\infty}^{+\infty}\int_{-\infty}^{+\infty} f(x,y)\delta(x\cos\theta+y\sin\theta-\rho)e^{-j2\pi\omega\rho}dxdyd\rho \\
&= \int_{-\infty}^{+\infty}\int_{-\infty}^{+\infty} f(x,y)\left[\int_{-\infty}^{+\infty}\delta(x\cos\theta+y\sin\theta-\rho)e^{-j2\pi\omega\rho}d\rho\right]dxdy \\
&= \int_{-\infty}^{+\infty}\int_{-\infty}^{+\infty} f(x,y)e^{-j2\pi\omega(x\cos\theta+y\sin\theta)}dxdy \\
&= \left[\int_{-\infty}^{+\infty}\int_{-\infty}^{+\infty} f(x,y)e^{-j2\pi(ux+vy)}dxdy\right]_{u=\omega\cos\theta;v=\omega\sin\theta} \\
&= \left[F(u,v)\right]_{u=\omega\cos\theta;v=\omega\sin\theta} \quad (F(u,v)\text{是}f(x,y)\text{的傅里叶变换}) \\
&= F(\omega\cos\theta,\omega\sin\theta)
\end{aligned}
$$

5.10 由投影重建图像

傅里叶切片定理

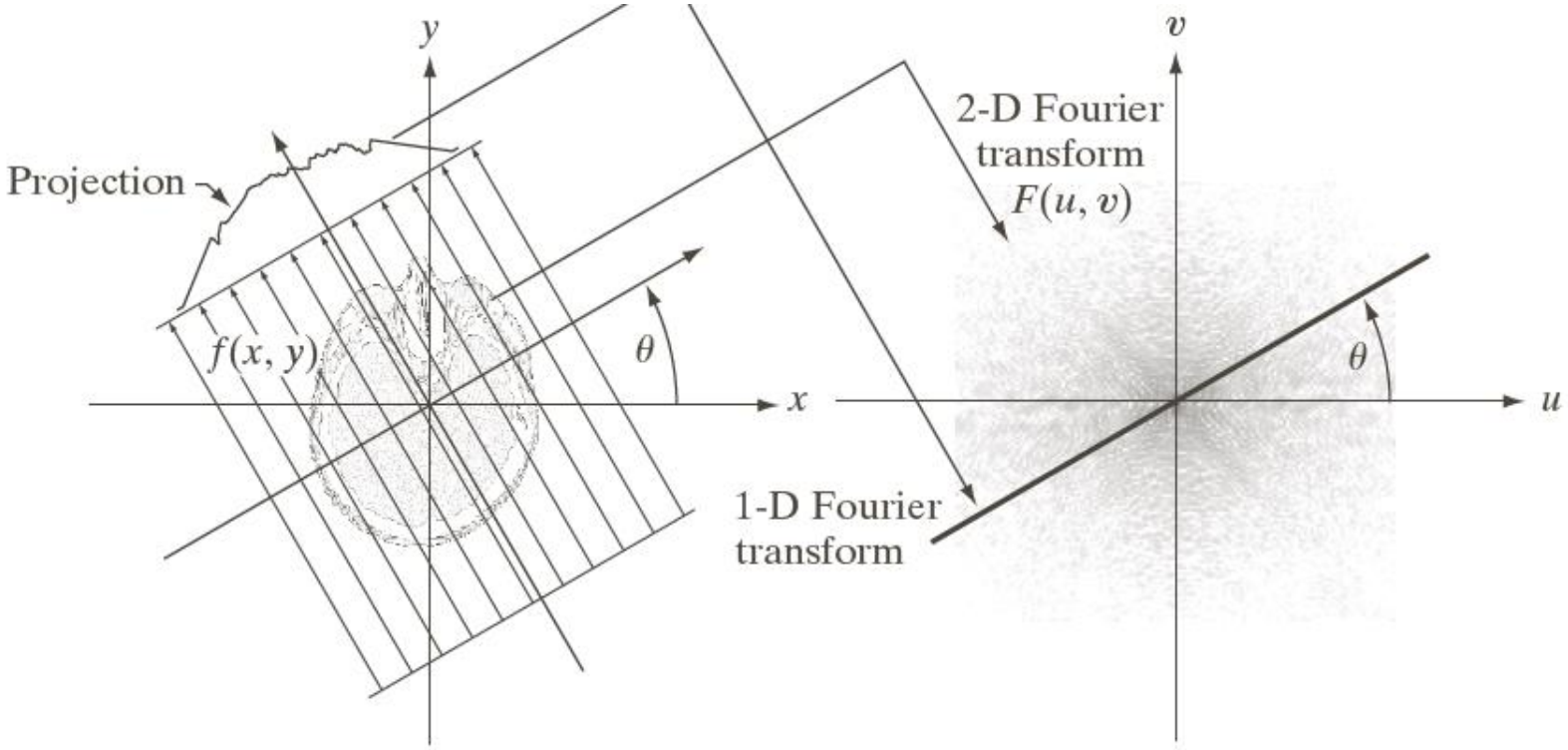

5.10 由投影重建图像

使用平行射线束滤波反投影的重建

$$f(x,y)=\int_{-\infty}^{+\infty}\int_{-\infty}^{+\infty}F(u,v)\mathrm{e}^{j2\pi(ux+vy)}dudv$$

$$=\int_{0}^{2\pi}\int_{0}^{+\infty}F\left(\omega\cos\theta,\omega\sin\theta\right)\mathrm{e}^{j2\pi\omega(x\cos\theta+y\sin\theta)}\,\omega d\omega d\theta\quad(u=\omega\cos\theta,v=\omega\sin\theta)$$

$$=\int_{0}^{2\pi}\int_{0}^{+\infty}G\left(\omega,\theta\right)\mathrm{e}^{j2\pi\omega(x\cos\theta+y\sin\theta)}\,\omega d\omega d\theta\qquad\left(F\left(\omega\cos\theta,\omega\sin\theta\right)=G\left(\omega,\theta\right)\right)$$

$$=\int_{0}^{\pi}\int_{-\infty}^{+\infty}|\omega|G\left(\omega,\theta\right)\mathrm{e}^{j2\pi\omega(x\cos\theta+y\sin\theta)}\,d\omega d\theta$$

$$=\int_{0}^{\pi}\left[\int_{-\infty}^{+\infty}|\omega|G\left(\omega,\theta\right)\mathrm{e}^{j2\pi\omega\rho}\,d\omega\right]_{\rho=x\cos\theta+y\sin\theta}d\theta$$

5.10 由投影重建图像

使用平行射线束滤波反投影的重建

a b
c d e

FIGURE 5.42
(a) Frequency domain plot of the filter $|\omega|$ after band-limiting it with a box filter. (b) Spatial domain representation. (c) Hamming windowing function. (d) Windowed ramp filter, formed as the product of (a) and (c). (e) Spatial representation of the product (note the decrease in ringing).

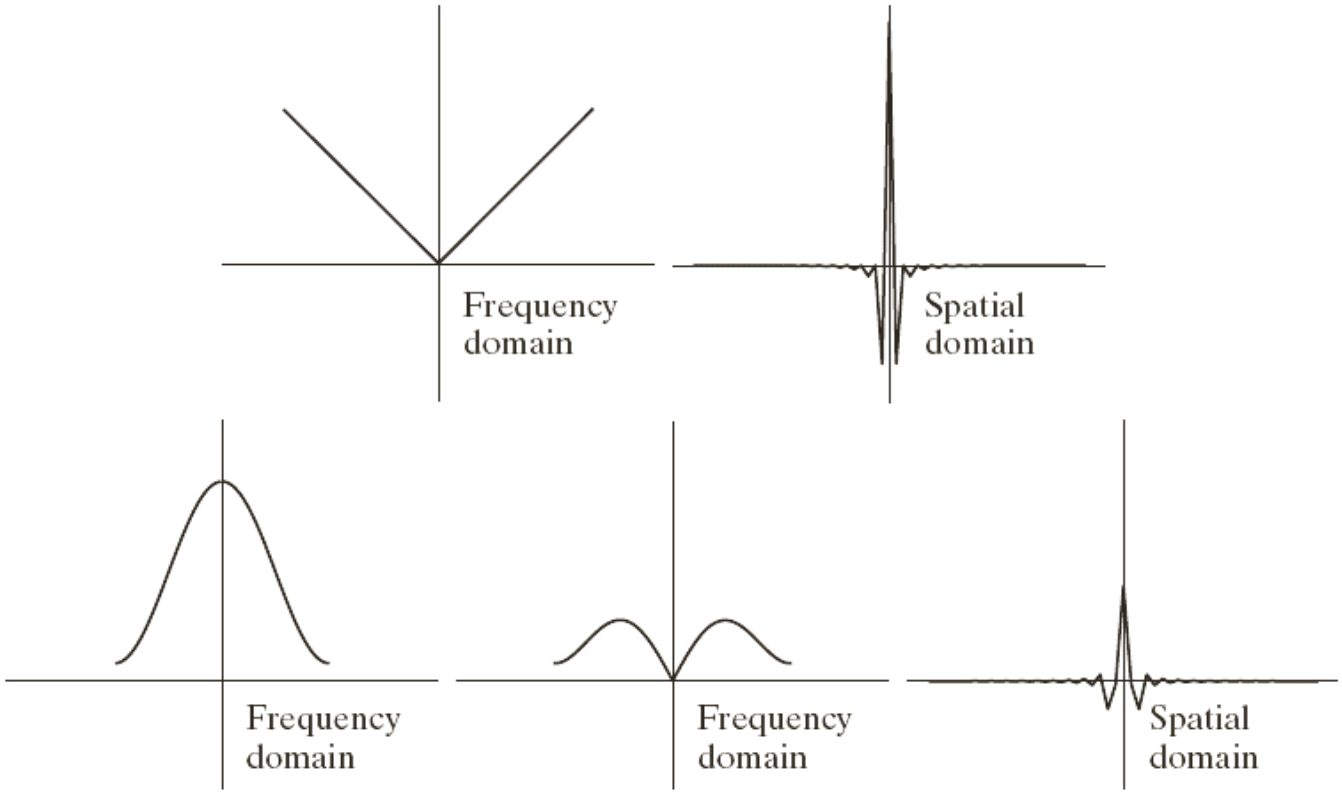

5.10 由投影重建图像

使用平行射线约束滤波反投影的重建

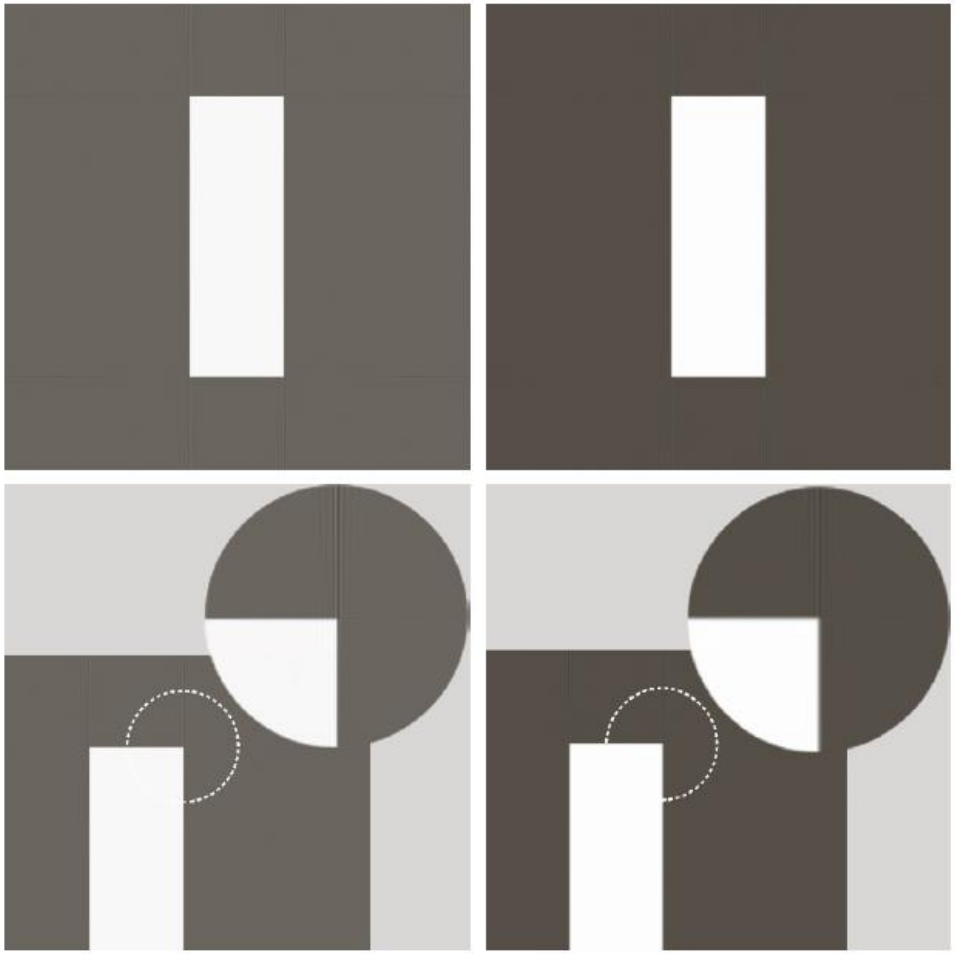

a b
c d

FIGURE 5.43
Filtered back-projections of the rectangle using (a) a ramp filter, and (b) a Hamming-windowed ramp filter. The second row shows zoomed details of the images in the first row. Compare with Fig. 5.40(a).

5.10 由投影重建图像

使用平行射线束滤波反投影的重建

a b

FIGURE 5.44
Filtered backprojections of the head phantom using (a) a ramp filter, and (b) a Hamming-windowed ramp filter. Compare with Fig. 5.40(b).

5.10 由投影重建图像

使用平行射线束滤波反投影的重建

$$f(x,y)=\int_0^{\pi}\left[\int_{-\infty}^{+\infty}|\omega|G(\omega,\theta)\mathrm{e}^{j2\pi\omega\rho}\,d\omega\right]_{\rho=x\cos\theta+y\sin\theta}d\theta$$

$$=\int_0^{\pi}\left[s(\rho)*\mathrm{g}(\rho,\theta)\right]_{\rho=x\cos\theta+y\sin\theta}d\theta$$

$$=\int_0^{\pi}\left[\int_{-\infty}^{+\infty}g(\rho,\theta)\mathrm{s}(x\cos\theta+y\sin\theta-\rho)d\rho\right]d\theta$$

5.10 由投影重建图像

使用平行射线约束滤波反投影的重建

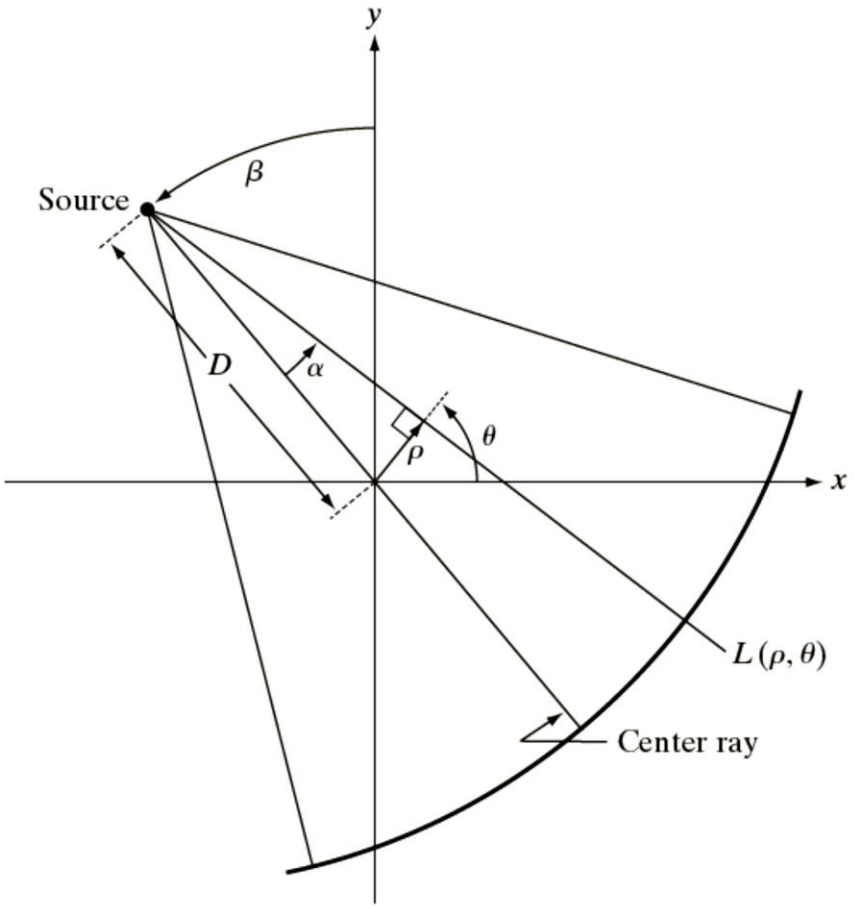

FIGURE 5.45
Basic fan-beam geometry. The line passing through the center of the source and the origin (assumed here to be the center of rotation of the source) is called the *center ray*.

5.10 由投影重建图像

使用扇形射线束滤波反投影的重建

$$f(x,y)=\frac{1}{2}\int_0^{2\pi}\left[\int_{-T}^{+T} g(\rho,\theta)\mathrm{s}(x\cos\theta+y\sin\theta-\rho)d\rho\right]d\theta$$

$$=\frac{1}{2}\int_0^{2\pi}\int_{-T}^{+T} g(\rho,\theta)\mathrm{s}\left[r\cos(\theta-\varphi)-\rho\right]d\rho d\theta$$

$$f(\mathrm{r},\varphi)=\frac{1}{2}\int_{\alpha}^{2\pi-\alpha}\int_{\arcsin(-\mathrm{T/D})}^{\arcsin(T/D)} g(D\sin\alpha,\alpha+\beta)\mathrm{s}\left[r\cos(\beta+\alpha-\varphi)-D\sin\alpha\right]Dd\alpha d\beta$$

$$=\frac{1}{2}\int_0^{2\pi}\int_{-\alpha_m}^{+\alpha_m} p(\alpha,\beta)\mathrm{s}\left[r\cos(\beta+\alpha-\varphi)-D\sin\alpha\right]Dd\alpha d\beta$$

5.10 由投影重建图像

使用扇形射线束滤波反投影的重建

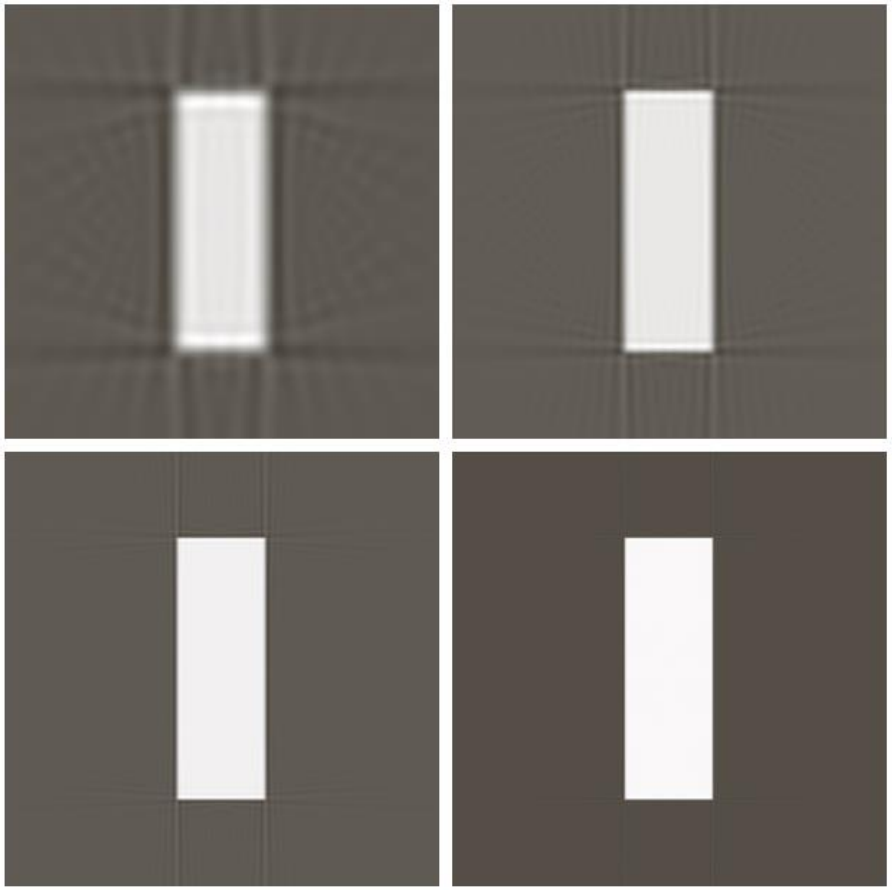

a b
c d

FIGURE 5.48
Reconstruction of the rectangle image from filtered fan backprojections. (a) 1° increments of α and β. (b) 0.5° increments. (c) 0.25° increments. (d) 0.125° increments. Compare (d) with Fig. 5.43(b).

5.10 由投影重建图像

使用扇形射线束滤波反投影的重建

a b
c d

FIGURE 5.49
Reconstruction of the head phantom image from filtered fan backprojections. (a) 1° increments of α and β. (b) 0.5° increments. (c) 0.25° increments. (d) 0.125° increments. Compare (d) with Fig. 5.44(b).